



HAL
open science

PaleoJump: A database for abrupt transitions in past climates

Witold Bagniewski, Denis-Didier Rousseau, Michael Ghil

► To cite this version:

Witold Bagniewski, Denis-Didier Rousseau, Michael Ghil. PaleoJump: A database for abrupt transitions in past climates. *Scientific Reports*, 2023, 13 (1), pp.4472. 10.1038/s41598-023-30592-1 . hal-04005934

HAL Id: hal-04005934

<https://hal.science/hal-04005934v1>

Submitted on 27 Feb 2023

HAL is a multi-disciplinary open access archive for the deposit and dissemination of scientific research documents, whether they are published or not. The documents may come from teaching and research institutions in France or abroad, or from public or private research centers.

L'archive ouverte pluridisciplinaire **HAL**, est destinée au dépôt et à la diffusion de documents scientifiques de niveau recherche, publiés ou non, émanant des établissements d'enseignement et de recherche français ou étrangers, des laboratoires publics ou privés.



Distributed under a Creative Commons Attribution 4.0 International License

PaleoJump: A database for abrupt transitions in past climates

Witold Bagniewski^{1,*}, Denis-Didier Rousseau^{2,3,4}, and Michael Ghil^{1,5}

¹Department of Geosciences and Laboratoire de Météorologie Dynamique (CNRS and IPSL), École Normale Supérieure and PSL University, Paris, France

²Geosciences Montpellier, University of Montpellier, CNRS, Montpellier, France

³Institute of Physics - CSE, Division of Geochronology and Environmental Isotopes, Silesian University of Technology, Gliwice, Poland

⁴Lamont-Doherty Earth Observatory, Columbia University, New York, USA

⁵Department of Atmospheric and Oceanic Sciences, University of California at Los Angeles, Los Angeles, USA

*wbagniewski@lmd.ipsl.fr

ABSTRACT

Tipping points (TPs) in Earth's climate system have been the subject of increasing interest and concern in recent years, given the risk that anthropogenic forcing could cause abrupt, potentially irreversible, climate transitions. Paleoclimate records are essential for identifying past TPs and for gaining a thorough understanding of the underlying nonlinearities and bifurcation mechanisms. However, the quality, resolution, and reliability of these records can vary, making it important to carefully select the ones that provide the most accurate representation of past climates. Moreover, as paleoclimate time series vary in their origin, time spans, and periodicities, an objective, automated methodology is crucial for identifying and comparing TPs. To address these challenges, we introduce the open-source PaleoJump database, which contains a collection of carefully selected, high-resolution records originating in ice cores, marine sediments, speleothems, terrestrial records, and lake sediments. These records describe climate variability on centennial, millennial and longer time scales and cover all the continents and ocean basins. We provide an overview of their spatial distribution and discuss the gaps in coverage. Our statistical methodology includes an augmented Kolmogorov-Smirnov test and Recurrence Quantification Analysis; it is applied here, for illustration purposes, to selected records in which abrupt transitions are automatically detected and the presence of potential tipping elements is investigated. These transitions are shown in the PaleoJump database along with other essential information about the records, including location, temporal scale and resolution, as well as temporal plots. This open-source database represents, therefore, a valuable resource for researchers investigating TPs in past climates.

Introduction and Motivation

Since the discovery of Dansgaard-Oeschger (DO) events in Greenland ice cores¹⁻³, climate research has aimed to identify other examples of centennial-to-millennial climate variability, including in marine and terrestrial paleoclimate records^{4,5}, and to gain insight into the mechanisms behind these changes. Many such records exhibit abrupt transitions, raising the question of whether similarly drastic changes may occur in the near future, as anthropogenic global warming pushes the climate system away from the relatively stable state that has persisted throughout the Holocene. Many of Earth's subsystems exhibit intrinsic variability and respond nonlinearly to various natural and anthropogenic forcings^{6,7}. Hence, any of these subsystems could experience a sudden shift into a new state once certain key thresholds, known as tipping points (TPs), are crossed⁸⁻¹⁰.

Identifying potential TPs in the climate system requires theoretical and modeling work, including comparison with observations. Proxy records of past climate and environmental changes play a crucial role, by enabling the reconstruction of Earth's climatic history. These records, particularly those that show abrupt transitions, may provide valuable insights into the past behavior of Earth's systems and possible TPs. By using this information, we can gain a better understanding of the possible trajectories of future climate change and their environmental impacts.

With tens of thousands of paleoclimate datasets available, finding and selecting the most relevant records for studying past climate can be overwhelming. These proxy datasets originate from different geologic structures, contain different variables, and span a wide range of age intervals with different resolutions. In addition, due to the varying resolution and dating methods used for these records, it is important to assess their reliability. There have been efforts in recent years to build compilations of high-quality paleoclimate data, such as the ACER database of pollen and charcoal records from the last glacial period¹¹, the SISAL database of speleothem isotope records¹², the PalMod compilation of marine sediment data covering the last glacial-interglacial cycle¹³, the World Atlas of late Quaternary Foraminiferal Oxygen and Carbon Isotope Ratios¹⁴, and the

34 PhanSST database of Phanerozoic sea surface temperature proxy data¹⁵. These compilations, however, are typically limited to
35 a specific type of proxy or time interval.

36 To fully understand TPs, which can affect various components of the earth system^{6,9,16} and have occurred at different times
37 in the past, it is essential to examine a diverse range of paleoclimate data. This includes marine, terrestrial, and ice records
38 from different time intervals during which abrupt climate change events have occurred, such as the Paleocene-Eocene Thermal
39 Maximum (PETM), DO events, and the Younger Dryas. Furthermore, as tipping elements — the subsystems that may be
40 subject to tipping — are interconnected, a potential for domino effects exists¹⁷. To identify and describe such effects in past
41 records, one needs coverage from different types of archives with a comprehensive geospatial distribution.

42 The purpose of this paper is to address these challenges by presenting the open-source PaleoJump database¹⁸,
43 <https://paleojump.github.io>, which compiles globally sourced high-resolution paleoclimate records that contain abrupt transitions.
44 The records originate in ice cores, marine sediments, speleothems, terrestrial deposits, and lake sediments, and can provide
45 valuable information for modeling and predicting critical TPs in current and future climate evolution. The database is designed
46 as a website, allowing easy access and navigation. It includes a map of the paleoclimate records, as well as tables that list
47 supplementary information for each record, along with dates of the detected transitions.

48 In addition to providing a description of the PaleoJump database, we demonstrate its potential use by conducting a
49 TP analysis of seven records selected from the database. Since paleoclimate records vary in their origin, time spans, and
50 periodicities, an objective, automated methodology is key for identifying and comparing TPs. Here, we apply a recently
51 developed method to detect abrupt transitions based on an augmented Kolmogorov-Smirnov (KS) test¹⁹ to the selected records.
52 The KS test results are then compared with those of recurrence quantification analysis (RQA)^{20,21} to further assess the validity
53 of the findings.

54 The next section describes the database itself, followed by a section summarizing the KS and RQA methods. Next, a section
55 illustrates the application of these two methods to the seven selected records, including comparisons between the results for
56 distinct records. The following section compares the results of the two methods and provides an interpretation of our findings.
57 Conclusions of the work follow in the last section.

58 Database sources

59 The PaleoJump database currently includes records from 131 sites, grouped by their geological type: 49 marine-sediment cores,
60 32 speleothems, 18 lake sediment cores, 20 terrestrial records, and 12 ice cores. The main sources for this database are the
61 PANGAEA and NCEI/NOAA open-access data repositories, while some records are, unfortunately, available only on request
62 from the authors of the original studies; in the latter case, links to the corresponding articles are provided. The paleorecords
63 have been selected for their ability to represent different aspects of past climate and environmental variability. In addition to
64 containing abrupt transitions, these records are characterized by high temporal resolution, multi-millennial time scales, and a
65 comprehensive spatial coverage. This selection simplifies the search for records that are most helpful in the investigation of
66 critical transitions and of the behavior of tipping elements.

67 Resolution is a crucial factor in the selection of records. As a metric, we use ‘maximum resolution’, which we define as the
68 temporal resolution of the 10 ky interval with the smallest average time step. We took this approach to ensure that records
69 with nonuniform resolution or with gaps in the data are not overlooked. To make the selection more conservative, we only
70 considered resolution for time intervals older than 14 ka BP because more recent intervals often have a significantly higher
71 resolution. The selection criteria varied depending on the source type and time interval. For example, for records that only
72 cover the Last Glacial Cycle, we select those with a maximum resolution of 200 years or better, while older records in our
73 database have a resolution no worse than 400 years. However, exceptions were made for records from undersampled regions,
74 such as the Guliya ice core²² and several lake sediment records, and for exceptionally long and complete records, like the
75 CENOGRID²³ and Chinese Loess Plateau²⁴ stacks.

76 While many of the paleosites listed in PaleoJump include multiple proxy types, we have focused on proxies that can be
77 directly compared with climate models: oxygen isotopes reflecting changes in past temperatures, sea level, and precipitation;
78 carbon isotopes containing information on past vegetation and the carbon cycle; aeolian deposits that include signatures of past
79 precipitation, mineral aerosols, and atmospheric transport patterns; as well as other proxy-based estimates of past temperatures.
80 We have mainly focused on the Last Glacial Cycle, due to the well-established evidence of past abrupt transitions — such as
81 DO and Heinrich events — with most records also covering Holocene deglaciation. Other records extend further back in time,
82 including DO-like events during earlier glacial cycles of the Quaternary, and earlier climatic events of the Cenozoic era, such as
83 the Eocene–Oligocene Transition at 34 Ma or the PETM at 56 Ma. While PaleoJump provides global coverage with records
84 from all continents and ocean basins, its spatial coverage is biased towards the North Atlantic region due to greater availability
85 and to the strong impact of the DO events.

86 The well-known uncertainties in paleoclimate records need to be considered in building such a database. A key source
87 of uncertainty is in their chronologies, as dating methods such as radiocarbon dating and layer counting have limitations and

88 potential sources of error^{25,26}. When independent dating is unavailable, “wiggle matching” is often performed to match records
89 with other, well-dated records, but this method’s use can be complicated by differences in local climate variability and time lags
90 in climate signal propagation^{27,28}. Additionally, recorded values of climate proxies may be affected by extra-climatic processes
91 — physical, biological, and chemical — or by measurement errors. Interpretation of proxy records can also be challenging
92 because a given proxy variable may be influenced by multiple climatic processes^{29–31}, making it difficult to determine the
93 specific climate conditions it represents.

94 In many of the records in PaleoJump, the chronology used for the original study has since been updated in more recent
95 ones. When this is the case, we use the most recent age model’s chronology. However, when the newer chronology does not
96 cover the complete record, which is often the case, we use the older chronology. Furthermore, we did not attempt to harmonize
97 and synchronize the age models among the records. These choices ensure that the most complete versions of the records are
98 included in the database, while also allowing users to independently reproduce our analyses without having to reevaluate how
99 harmonization was performed.

100 Five tables show the information for each record in the PaleoJump database and are included in the Supplementary
101 Information^{4,5,11,22–24,32–174}.

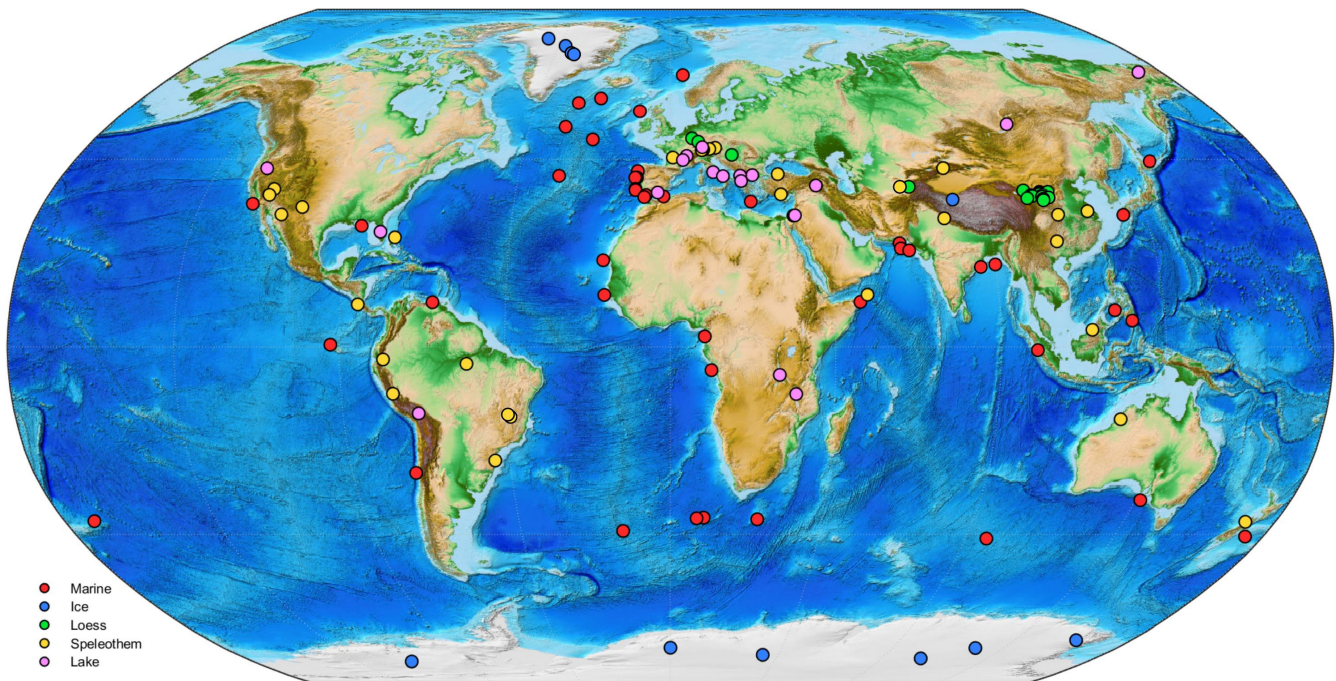


Figure 1. Map of the records included in the PaleoJump database and listed in the Supplementary Information. The five record sources — marine sediments, ice cores, terrestrial deposits, speleothems, and lake sediments — are identified in the legend by color.

102 Applying the KS test and RQA to TP identification

103 Given the diversity of the proxy records in the PaleoJump database, an objective, automated methodology is crucial for
104 identifying and comparing TPs. Bagniewski et al.¹⁹ formulated an augmented KS test, which they used to robustly detect and
105 identify abrupt transitions during the last glacial cycle. These results were compared with results obtained using RQA, showing
106 that the two methods are complementary, with KS test being more useful at detecting individual jumps and determining their
107 exact dates, while RQA can help establish important transitions in a record’s characteristic time scale. Here, we apply these
108 two methods to a selection of records from the PaleoJump database and demonstrate the ability of the augmented KS test to
109 accurately identify transitions in various types of paleoclimate records.

110 **Kolmogorov-Smirnov (KS) test.** The augmented KS methodology¹⁹ is based on the nonparametric KS test¹⁷⁵. A two-sample
111 KS test is applied to two neighboring samples drawn from a proxy time series within a sliding window of length w . The
112 commonality of the two samples is quantified by the the KS statistic D_{KS} ^{175,176}. A “jump” in the time series is identified at any
113 point in time at which D_{KS} is greater than a cut-off threshold D_c . As the KS test can give very different results depending on

the window length w being used, D_{KS} is calculated for different w 's, varying between w_{\min} and w_{\max} . The values of the latter two parameters bracket the desired time scale at which a given paleorecord is to be investigated. Furthermore, smaller jumps in the time series may be the result of an error in the observed data or small-scale variability that occurs over time intervals shorter than the sampling resolution of the proxy record and they should be discarded. Thus, for a transition to be considered significant, the change in magnitude between the two samples (i, j) should exceed a threshold σ_c in their standard deviations (σ_i, σ_j) . Finally, as the KS test requires a large enough sample size to be significant, its results are rejected if either of the two samples has a size n smaller than n_c .

At a time step at which all three conditions based on the parameters D_c , σ_c , and n_c are satisfied, an abrupt transition is identified. As the dates of such transitions often occur in clusters, the precise date for a transition within such a cluster is determined by the maximum D_{KS} value found within the corresponding time interval. When the maximum D_{KS} over a given interval is shared by several time steps, the one corresponding to the maximum change in absolute magnitude is used; moreover, if there are several jumps of equal amplitude, then the one with the earliest date is used.

As the same transition may be found at slightly different dates depending on the window length that is used, we first identify the transitions detected with the longest window, which, given the larger sample size it accommodates, is the most statistically significant one. These transitions are then supplemented by those detected for the next-longest window and eventually for all other window lengths. For window w_i , we discard transitions identified at time t if the interval $\{t - w_i \leq t \leq t + w_i\}$ contains transitions that were previously identified with a greater window length. Finally, to identify transitions between dominant climate modes, such as the Stadial-Interstadial (GS – GI) boundaries, we use a running window to extract the upper and lower values from the time series and locate the transitions that mark a shift from one mode to the other.

The parameters D_c and σ_c are initially optimized following receiver operating characteristic analysis^{177,178}, and abrupt transitions so identified for the NGRIP ice core $\delta^{18}\text{O}$ record are further compared with the change points identified using visual inspection by Rasmussen *et al.*¹³¹.

Recurrence Quantification Analysis (RQA). The KS test results are next compared with RQA results^{20,21,179}. Here, the Recurrence Plot (RP) for a time series $\{x_k : k = 1, \dots, K\}$ is given by a square pattern in which both axes represent time. A dot is entered into a position (i, j) of the matrix \mathbf{R} when $|x_i - x_j| < \varepsilon$, with ε being the recurrence threshold. Thus, the RP appears as a square matrix \mathbf{R} of dots. For details on how ε is determined, see Marwan *et al.*²¹ and Bagniewski *et al.*¹⁹.

Eckmann *et al.*²⁰ showed that purely visual RP typologies provide useful information about a time series. However, RQA allows for a more objective way of inferring recurrence^{21,179}, by quantifying selected recurrence characteristics. One of the simplest RQA criteria is the recurrence rate (RR), namely the density of dots within the recurrence plot: RR describes the probability of states of the system recurring within a particular time interval. By evaluating RQA measures such as RR in a sliding window, it is possible to identify changes in the time series. Low RR values correspond to an unstable behavior of the system, and hence abrupt transitions in a time series may be identified by local RR minima.

An important advantage of the recurrence method is that it does apply to dynamical systems that are not autonomous, i.e., that may be subject to time-dependent forcing²⁰. The latter is certainly the case for the climate system in general^{180–183} and, in particular, on the time scales of 10–100 kyr and longer, which are affected strongly by orbital forcing¹⁸⁴.

For a more comprehensive description of both the augmented KS test and RQA, see Bagniewski *et al.*¹⁹.

Examples of usage

Here we show the results of the augmented KS test methodology¹⁹, as applied to records of different timescales, resolutions, and periodicities. Plots of the detected transitions, along with files listing their dates are included in the PaleoJump database; the same is available for other records as well.

Methodology. We apply the augmented KS test to six records, given in Table 1, from each of the proxy types listed in Supplementary Tables 1–5. In addition to these six records, we include the results obtained for the NGRIP ice core, which have been published in Bagniewski *et al.*¹⁹, and compare the latter with the three records of the last glacial cycle in the table, to wit MD03-2621, Paraiso Cave, and ODP893A.

Type	Site name	Location	Depth/elevation	Age	Res.	Proxy
Marine	ODP893A ^{87,88}	34.28, -120.03	576 m	65 - 0 ka	41 y	pla $\delta^{18}\text{O}$
Marine	MD03-2621 ⁶⁴	10.678, -64.972	847 m	109 - 6 ka	0.1 y	reflectance
Marine	U1308 ⁹⁵	49.878, -24.238	3871 m	3143 - 0 ka	118 y	ben $\delta^{18}\text{O}$
Marine	CENOGRID ²³	N/A	N/A	67.1 - 0 Ma	2000 y	ben $\delta^{18}\text{O}$
Terrestrial	Paraiso (PAR07) ¹⁶⁵	-4.067, -55.45	60 m	45 - 18 ka	21 y	$\delta^{18}\text{O}$

Type	Site name	Location	Depth/elevation	Age	Res.	Proxy
Terrestrial	Lake Ohrid ¹³⁷	41.049, 20.715	693 m	1.36 - 0 Ma	208 y	TIC
Ice	NGRIP ¹³¹	75.1, -42.32	2925 m	122 - 0 ka	20 y	$\delta^{18}\text{O}$

Table 1. Records analyzed using the augmented KS test¹⁹, ordered by geological type and temporal scale; the nature of the records is indicated in the last column by the abbreviations ben = benthic, pla = planktonic, and TIC = Total Inorganic Carbon.

The KS test parameters vary depending on a record's time resolution and on the length of its age interval. For the records covering the last glacial cycle (MD03-2621, Paraiso Cave, and ODP893A), we use the same parameter values as used for the NGRIP record in Bagniewski et al.¹⁹, i.e., $D_c = 0.77$, $\sigma_c = 1.9$, $n_c = 3$, $w_{\min} = 0.1$ kyr, and $w_{\max} = 2.5$ kyr. For the records spanning longer time intervals with a lower temporal resolution, we use longer window lengths w_{\min} and w_{\max} , thus shifting the focus of our analysis to longer time scales. For the U1308 benthic $\delta^{18}\text{O}$ and Lake Ohrid TIC records, we use a w -range of 2 kyr to 20 kyr. This allows us to focus on the glacial-cycle variability, as the record's resolution is too low to properly identify DO events, particularly for data older than 1.5 Ma BP, when the U1308 record's resolution is lower than for more recent data. For the CENOGRID record, we perform two separate analyses, one with a w -range of 1 Myr to 4 Myr to determine the Quaternary's major climatic shifts, and one with a w -range of 0.02 Myr to 2.5 Myr, which covers the orbital time scale. Note that, in paleoclimate studies, one distinguishes between units of absolute time, such as kyr or Myr, and units of age, such as ka BP or Ma BP, where 'BP' stands for "before present."

Results for Individual records. We chose the MD03-2621 reflectance record from the Cariaco Basin in the Caribbean for having a very high resolution and for its importance in studying the effect of DO events on the migrations of the intertropical convergence zone (ITCZ). The record is shown in Fig. 2 and it has been used previously to assess teleconnections between the North Atlantic basin and the Arabian Sea⁶⁴. When the ITCZ migrates southward during stadials, northeasterly Trade winds lead to upwelling of cool, nutrient-rich waters in the Caribbean; as the ITCZ migrates northward during interstadials, heavy convective rainfall leads to increased runoff from South America's north coast, delivering detrital material to the Cariaco Basin^{64,185}. As a result, the color reflectance in the core alternates between light-colored sediments, rich in foraminiferal carbonate and silica, and darker sediments abundant in detrital organic carbon. These changes in the marine sediments are proxies for the prevailing atmospheric circulation regime, and the meridional position of the ITCZ in the region, which are both linked to the glacial-interglacial variability.

For the KS analysis, a 20-year moving average of the MD03-2621 record is calculated in order to align its resolution with that of the NGRIP record. Our analysis does identify the "classical" DO events, as seen in the NGRIP record^{19,131}. There is, however, no direct relationship in the identified longer-scale warm (grey bars) and cool intervals: For instance, some events appear to be merged in Fig. 2, e.g., GI-23 and 22, GI-16 and 15, GI-14 and 13, GI-10 and 9, and GI-4 and 3, while some events detected here, between 68 and 66 ka BP, are not identified in NGRIP, and GI-2 is much longer than in NGRIP.

The RQA analysis^{21,179}, shown in Fig. 3, does identify the major transitions in the MD03-2621 reflectance record, including the relative significance of each. It does not, however, resolve smaller transitions that occur at the centennial time scale. Please see Bagniewski et al.¹⁹ for the explanation of the recurrence rate used to identify the transitions in the figure's panel (c).

The CENOGRID stack of benthic $\delta^{18}\text{O}$ ²³ shown here in Fig. 4 is a highly resolved 67 Myr composite from 14 marine records. Westerhold et al.²³ distinguished four climate states — Hothouse, Warmhouse, Coolhouse, and Icehouse — in this record, largely following changes in the polar ice volume. The composite in the figure²³ reconstructs in detail Earth's climate during the Cenozoic era, at a higher time resolution than the earlier compilation of Zachos and colleagues¹⁸⁶.

Our KS analysis in Fig. 4a uses a window width $1 \leq w \leq 4$ Myr and it identifies four major transitions towards higher $\delta^{18}\text{O}$ values and two towards lower ones. The oldest transition, at 58 Ma BP, is characterized by a shift from the moderately warm climate prevailing at the beginning of the Cenozoic to the hot conditions marked by the Early Eocene Climate Optimum between 54 Ma and 49-48 Ma BP. The second transition corresponds to the short but intense warm event known as the PETM, the Cenozoic's hottest one. The third transition marks the end of this hot interval and the return to the milder and relatively stable conditions that prevailed between 67 Ma and 58 Ma BP.

The fourth transition, at 34 Ma, is the Eocene–Oligocene Transition, the sharp boundary between the warm and the hot climatic conditions in the earlier Cenozoic and the Coolhouse and then Icehouse conditions prevailing later on¹⁸⁷. As this transition marks a major shift in the Earth's climate dynamics, it is a candidate for a major TP in Earth's climate history¹⁸⁸. The fifth transition, at 14 Ma BP, ends a rather stable climate interval between 34 Ma and 14 Ma, characterized by the build up of the East Antarctic ice sheet^{189,190}. This transition also marks the start of an increasing trend in benthic $\delta^{18}\text{O}$ values^{191,192}. The final transition marks the start of the Icehouse world and it is characterized by the emergence and development of the Northern Hemisphere ice sheets.

Using a reduced window length on the last 26 Myr of the CENOGRID benthic record, many more abrupt transitions are detected in Fig. 4b. In particular, higher variability in the $\delta^{18}\text{O}$ signal and much more frequent transitions are found during two

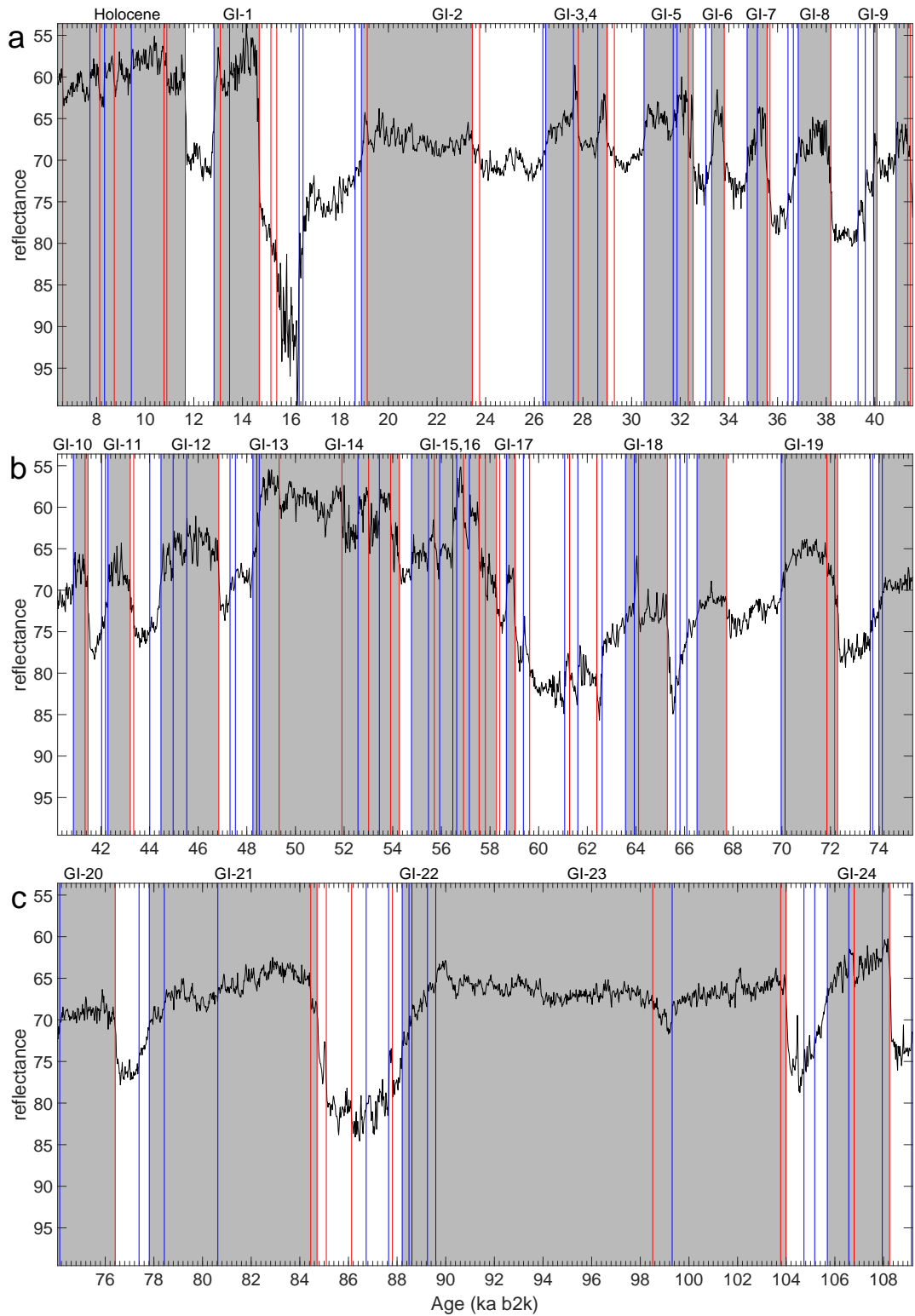


Figure 2. MD03-2621 marine sediment core: (a) 6.4–41.6 ka b2k; (b) 40.2–75.4 ka b2k; and (c) 74–109.2 ka b2k. The black solid line is the core reflectance⁶⁴, with the vertical axis reversed. Vertical lines represent transitions detected by the KS test of Bagniewski et al.¹⁹, with colors indicating the direction of the jumps. In this figure, red lines represent a warming event, while blue lines represent a cooling event. In other figures, the meaning of the colors may vary. Grey bars denote warm episodes. Note that all time axes in this paper follow the geological custom of pointing into the past.

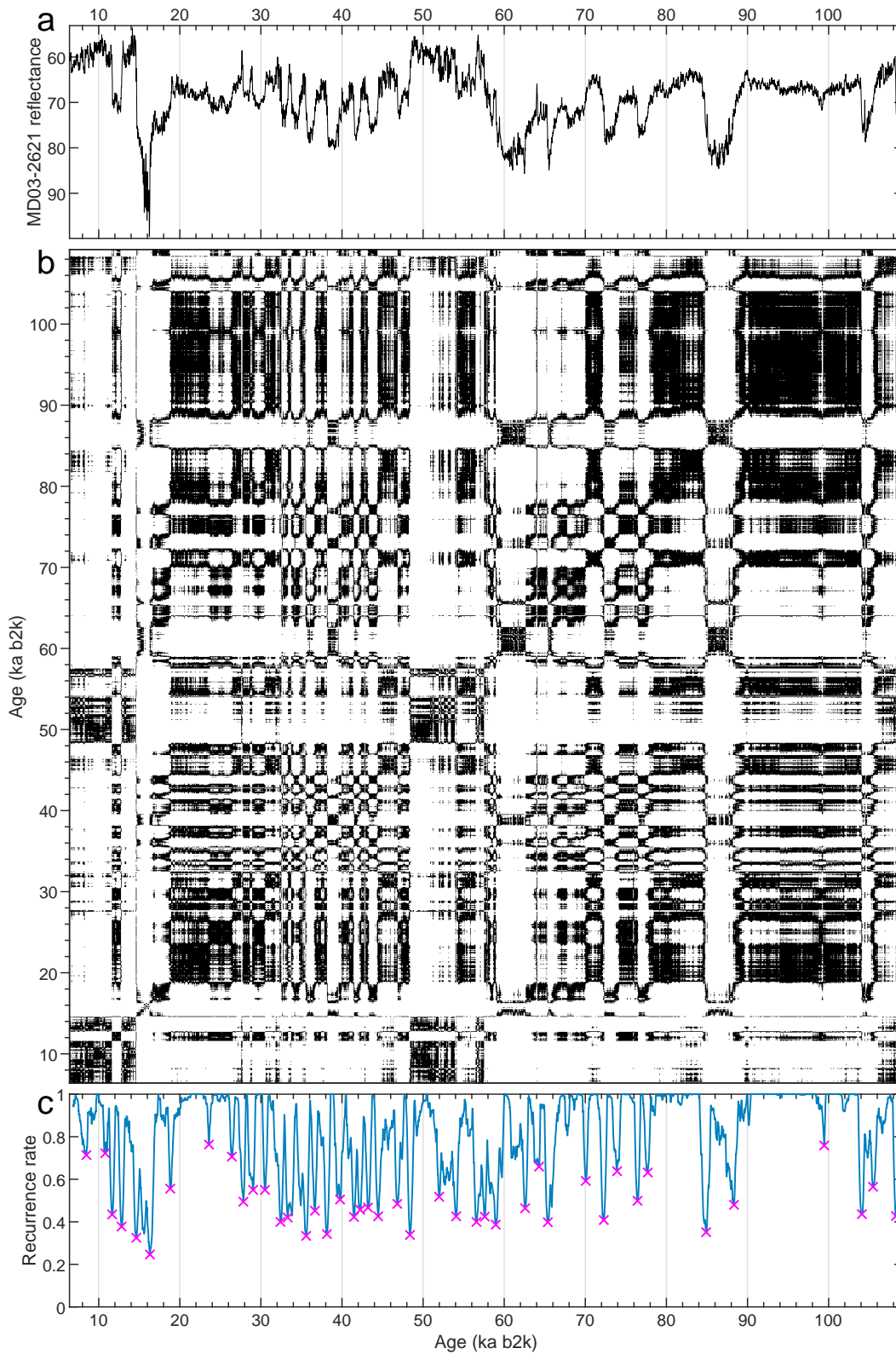


Figure 3. Recurrence Quantification Analysis (RQA)^{21,179} for the MD03-2621 reflectance record⁶⁴. (a) Time series with vertical axis as in Fig. 2; (b) recurrence plot (RP); and (c) recurrence rate. Magenta crosses in panel (c) represent the transitions identified by the RQA.

207 intervals, namely 71 transitions over the last 3.5 Myr and 77 transitions between 20 Ma BP and 13 Ma BP. In contrast, the
 208 intervals 67–20 Ma BP and 13–3.5 Ma BP are characterized by a lower frequency of detected transitions, with 112 and 13
 209 transitions, respectively. The former one of the two intervals with many jumps includes the Quaternary Period, which started
 210 2.6 Myr ago and is well known for its high climate variability, due to the presence of large ice masses in the system^{6,193}.

211 The interval 20–13 Ma BP, on the other hand, coincides with the exclusive use of the U1337 and U1338 records in
 212 constructing the CENOGRID stack, both of which are located in the eastern tropical Pacific. Higher sedimentation rates in
 213 these two cores might contribute to the higher variability $\delta^{18}\text{O}$ observed in the stack record over this interval. For transitions
 214 detected with the shorter window for the entire CENOGRID stack, please see Fig. S1 in the Supplementary Information.

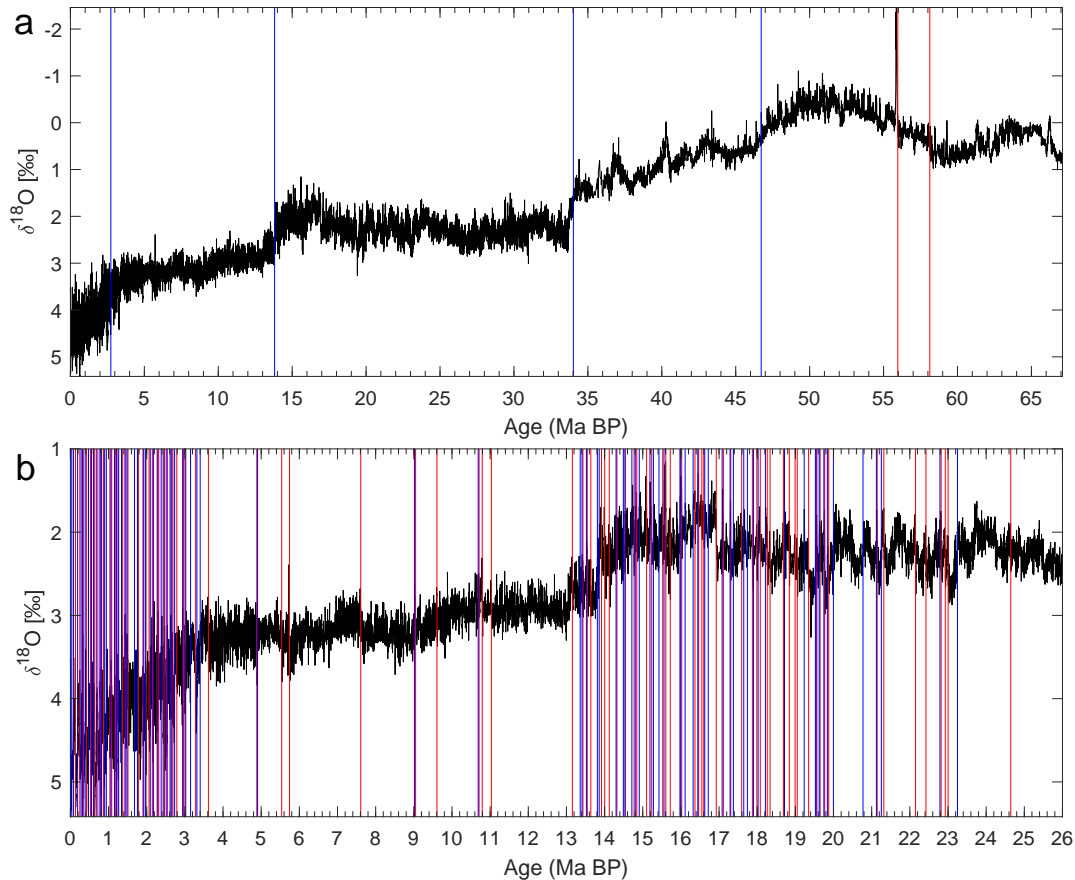


Figure 4. CENOGRID stack of benthic $\delta^{18}\text{O}$ ²³. Vertical lines represent transitions detected by the KS test¹⁹, with colors indicating the direction of the jumps. Grey bars represent warm episodes. (a) Transitions detected for the entire record using a window w range of 1 to 4 Myr, and (b) transitions detected for the interval 26–0 Ma BP using a w range of 0.02 to 2.5 Myr; see also the earlier subsection on “Methodology.” The vertical axes are reversed.

215 The $\delta^{18}\text{O}$ record from the Paraiso Cave in the Amazon rainforest reveals a relationship between shifts in global temperature
 216 and changes in rainfall patterns in the region; see Fig. 5. The record shows that the Amazon basin experienced drier conditions
 217 during the last glacial period, most probably due to the lower temperatures. The record exhibits reduced precipitation during DO
 218 interstadials and increased precipitation during stadials, a pattern that negatively correlates with Chinese speleothem records⁵⁵,
 219 suggesting a phase opposition in rainfall between the two regions. The abrupt shifts in precipitation during DO events suggest
 220 that the Amazonian climate subsystem may exhibit bistability, making it a potential tipping element as changes in precipitation
 221 may lead to forest dieback¹⁹⁴.

222 **Results for core intercomparisons.** In Fig. 6, we compare four paleorecords of different types and from distinct locations:
 223 NGRIP $\delta^{18}\text{O}$, MD03-2621 reflectance, Paraiso Cave $\delta^{18}\text{O}$, and ODP893A planktic $\delta^{18}\text{O}$ from the Santa Barbara Basin.
 224 Overall, the abrupt transitions in the four records appear to be fairly synchronous, with the main Greenland DO events from
 225 NGRIP also observed for the two marine records and the one speleothem record. The transitions that correspond to Greenland
 226 interstadials (GIs) GI-12 to GI-3¹³¹ are identified in all four records, with only a few exceptions: GI-3 is not identified for the
 227 ODP893A record, due to an insufficient number of data points; and GI-5.1 is not identified in any record, except as a cooling

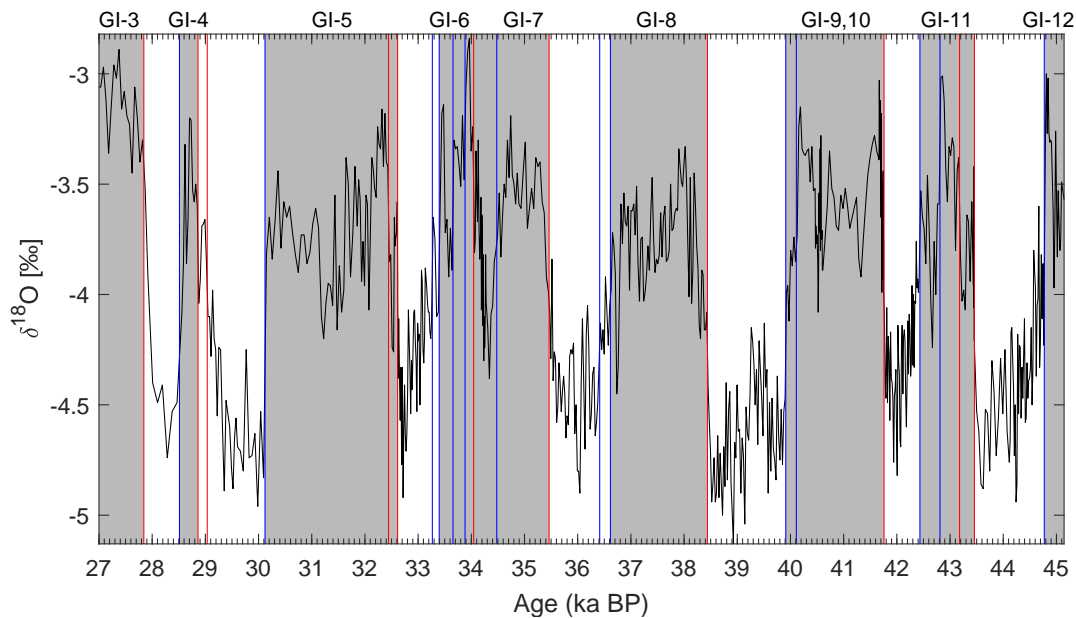


Figure 5. Paraiso Cave (PAR07) $\delta^{18}\text{O}$ ¹⁶⁵. Vertical lines represent transitions detected by the KS algorithm¹⁹, with colors indicating the direction of the jumps. Grey bars represent dry interglacial conditions.

228 event in MD03-2621 and in Paraiso cave. Also, GI-10 and GI-9 appear as a single interstadial in the Paraiso cave and ODP893A
 229 records, which is probably due to a decreased time resolution observed in both records during this time interval.

230 Finally, Fig. 7 shows the comparison between the U1308 benthic $\delta^{18}\text{O}$ record and the Lake Ohrid Total Inorganic Carbon
 231 (TIC) record over a 1.4 Myr time interval that includes multiple glacial-interglacial transitions.

232 The U1308 benthic $\delta^{18}\text{O}$ record in panel (a) of the figure is a 3.1 Myr record located within the ice-rafted detritus belt of
 233 the North Atlantic¹⁹⁵. This record is a proxy for deep-water temperature and global ice volume, and it has enabled a detailed
 234 reconstruction of the history of orbital and millennial-scale climate variability during the Quaternary; it documents the changes
 235 in Northern Hemisphere ice sheets that follow the glacial–interglacial cycles, as well as mode transitions identified at 2.55 Ma,
 236 1.5 Ma, 1.25 Ma, 0.65 Ma and 0.35 Ma BP^{95,196}. Here, we only show the 1.4–0 Ma BP time interval that corresponds to the
 237 length of the Lake Ohrid record. For the full 3.1 Myr U1308 record, please see Fig. S2 in the Supplementary Information.

238 The 1.25–0.65 Ma BP interval in the figure corresponds to the Mid-Pleistocene Transition, characterized by an increase
 239 in the amplitude of the glacial–interglacial fluctuations and a shift from a predominantly 40 kyr to a predominantly 100 kyr
 240 periodicity; see Reichers et al.¹⁸⁴ and references therein. The abrupt transition at 0.35 Ma marks the start of the strongest
 241 interglacial of the record, which corresponds to the marine isotope stage (MIS) 9. Here, our KS analysis agrees with the well
 242 established marine isotope stratigraphy of Lisiecki and Raymo¹⁹⁷ by detecting rapid warmings that correspond to the classical
 243 terminations leading to interglacials, as well as rapid coolings that initiate glacial stages.

244 The Lake Ohrid TIC record in Fig. 7b shows glacial–interglacial variability in biomass over the past 1.4 Myr. Here, our
 245 KS analysis shows numerous abrupt transitions towards high TIC intervals that correspond to interglacial episodes, as well as
 246 matching ones of opposite sign. The interglacials are associated with forested environmental conditions that are consistent
 247 with odd-numbered MISs, as was the case for the U1308 record in the figure’s panel (a). The glacial episodes, to the contrary,
 248 correspond to forestless conditions, that, according to the available timescale, are consistent with even-numbered MISs.

249 Discussion

250 **The two methods.** The augmented KS test of Bagniewski et al.¹⁹ has detected abrupt transitions on different time scales in a
 251 variety of paleorecords. These include the NGRIP ice core, the Paraiso Cave speleothem, and the MD03-2621 and ODP893A
 252 marine sediment cores for the last glacial cycle; the U1308 marine sediment core and Lake Ohrid TIC for the Middle and Late
 253 Pleistocene; and the CENOGRID marine sediment stack for the Cenozoic Era. While possible mechanisms giving rise to the
 254 observed variability in these records have been discussed in previous studies, the objective, precise and robust dating of the
 255 main transitions using the augmented KS test may allow a more detailed and definitive analysis and modeling.

256 The transitions identified for the MD03-2621 reflectance record with the RQA methodology^{20,21,179} do correspond to a
 257 subset of those found with the KS test, but several smaller-scale transitions identified by the latter have not been found with the

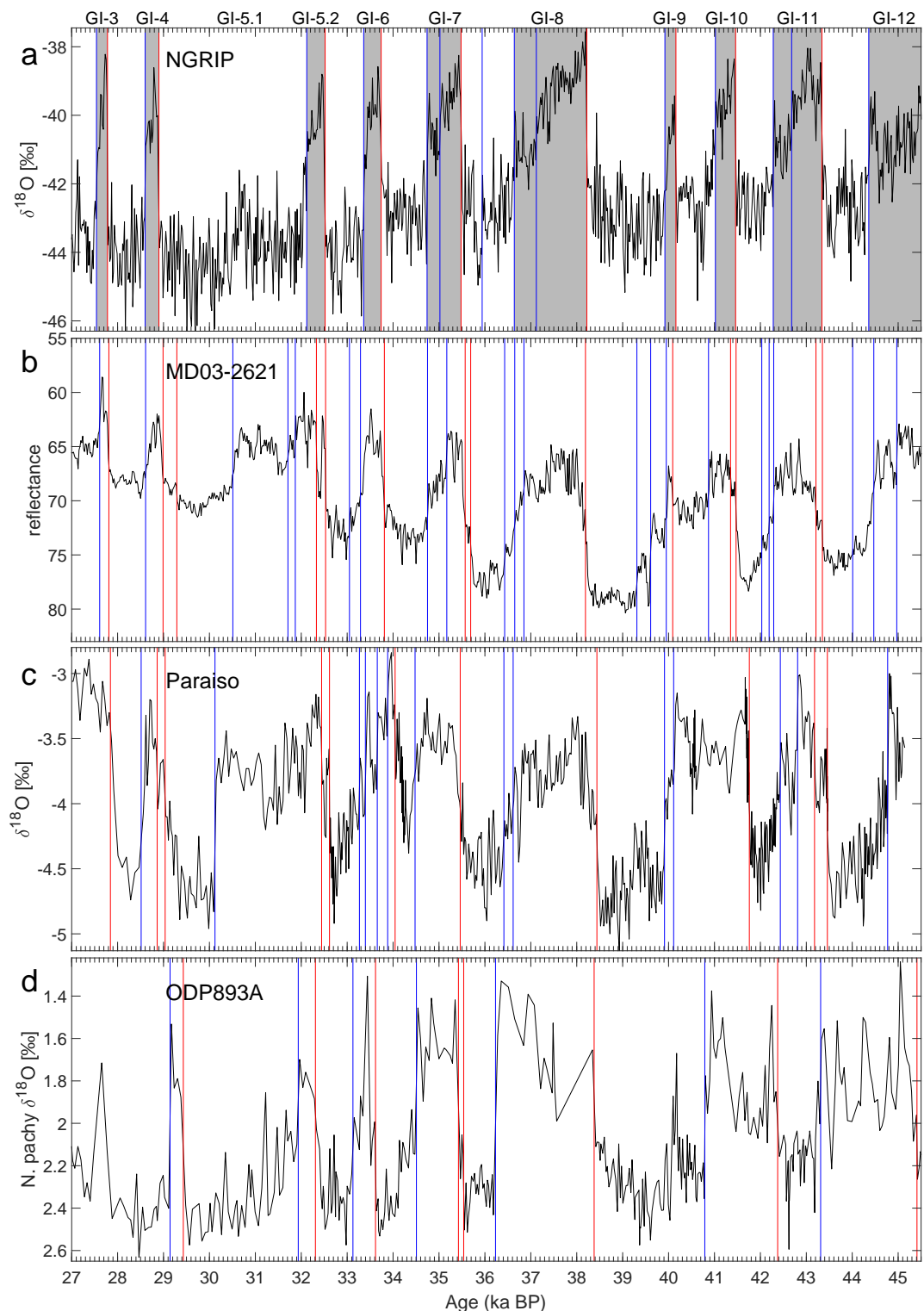


Figure 6. Comparison of four paleorecords over the 45.5 – 27 ka BP interval: (a) NGRIP ice core $\delta^{18}\text{O}^{131}$; (b) MD03-2621 marine sediment reflectance⁶⁴; (c) Paraiso Cave (PAR07) $\delta^{18}\text{O}^{165}$; and (d) ODP893A marine sediment *N. pachyderma* $\delta^{18}\text{O}^{87,88}$. Vertical lines represent detected transitions, with colors indicating the direction of the jumps. Grey bars in panel (a) represent interstadials identified for the NGRIP $\delta^{18}\text{O}$ record by Bagniewski et al.¹⁹. Note that the “ka BP” time unit, where the ‘Present’ is defined as the year 1950, applies only to the Paraiso and ODP893A records. The NGRIP and MD03-2621 records use the “ka b2k” time scale, where ‘b2k’ refers to the year 2000 as the origin of past times. The vertical axes in panels (b) and (d) are reversed.

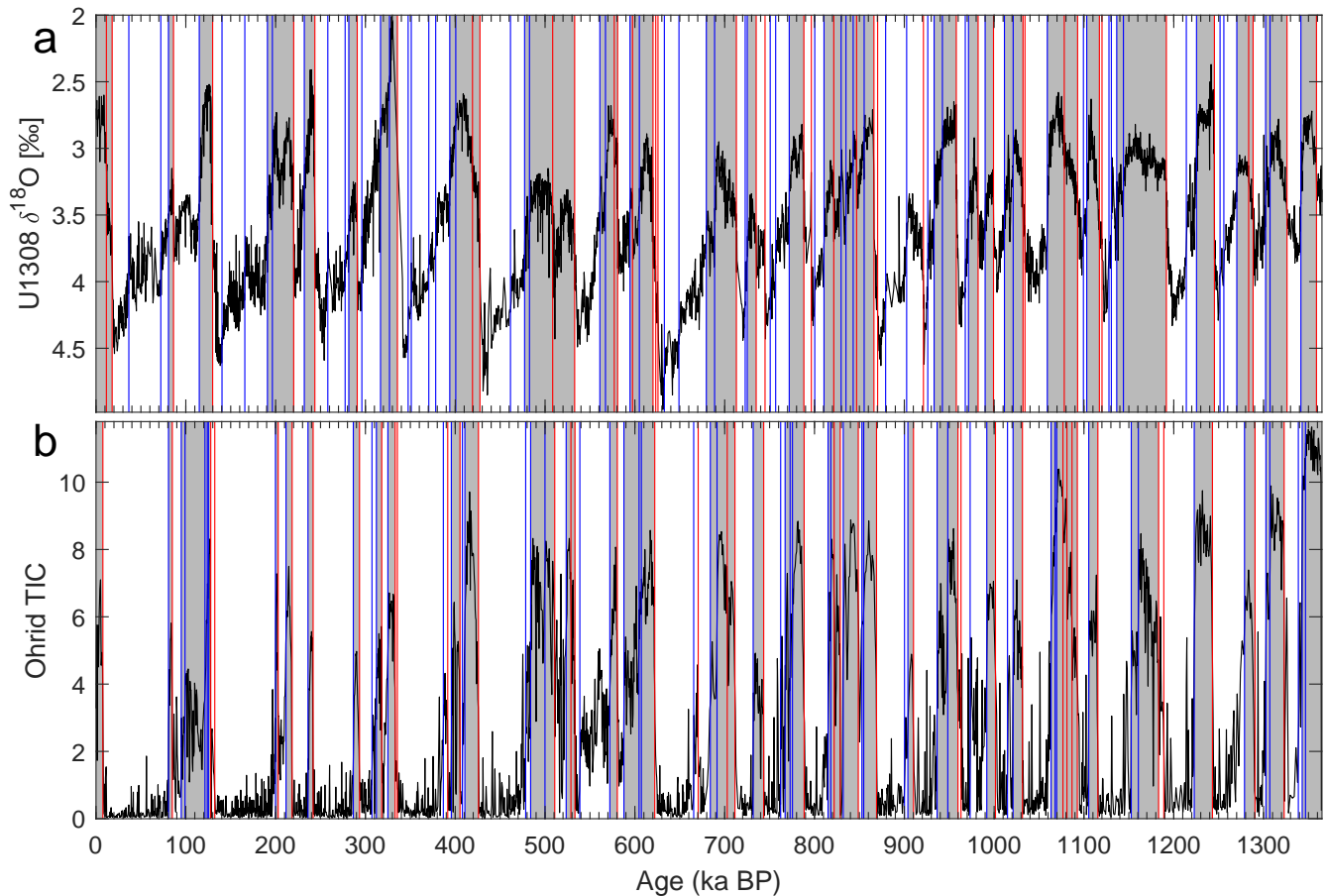


Figure 7. Comparison of the benthic *Cibicidoides* sp. $\delta^{18}\text{O}$ record in (a) the U1308 marine-sediment core⁹⁵ and (b) Lake Ohrid TIC¹³⁷. Vertical lines represent transitions detected by our KS methodology¹⁹, with colors indicating the direction of the jumps. Grey bars correspond to interglacials (odd-numbered MISs) and white bars correspond to glacials (even-numbered MISs). The vertical axis in panel (a) is reversed.

258 former method. As discussed in Bagniewski et al.¹⁹, recognizing the transition points by RQA becomes increasingly difficult at
 259 time scales shorter than the window length. The RQA approach, though, does allow one to quantify the magnitude of each
 260 transition, and it may thus be useful for identifying key transitions. Moreover, RPs may be helpful in illustrating changes in
 261 periodicity.

262 **Interpretation of findings.** The high-resolution MD03-2621 reflectance record from the Cariaco Basin⁶⁴ in Fig. 2 shows
 263 abrupt transitions that are largely in agreement with those detected by our KS test for the NGRIP record. Desplazes et al.⁶⁴ have
 264 argued that these transitions are driven by the ITCZ displacements that occurred primarily in response to Northern Hemisphere
 265 temperature variations. These authors indicated that the ITCZ migrated seasonally during mild stadials, but was permanently
 266 displaced south of the Cariaco Basin during the colder stadial conditions. The very high resolution of the MD03-2621 record
 267 allows a detailed comparison with the transitions identified for the NGRIP record. The fact that several small-scale NGRIP
 268 transitions are not identified by our KS test in the MD03-2621 record suggests that a TP linked to ITCZ migration was not
 269 crossed during these events. Furthermore, the KS test does reveal transitions that have not been recognized previously in either
 270 record¹³¹, e.g., at 86.15 ka BP, which we find in both the NGRIP and MD03-2621 records.

271 In the 67-Myr CENOGRID stack (Fig. 4) of benthic $\delta^{18}\text{O}$ ^{23,186}, we identified four major cooling transitions that culminate
 272 with the start of the Pleistocene, as well as two warming transitions, including the PETM. These major jumps agree with
 273 those identified in Westerhold et al.²³. However, using a shorter window length, many more transitions were detected during
 274 the Pleistocene, well known for its higher climate variability^{6,193}, as well as during the early Miocene, i.e., between the
 275 Oligocene-Miocene transition at 23 Ma BP^{198–200} and the mid-Miocene transition at 14 Ma BP¹⁹⁰. A possible reason is the fact
 276 that the 20–13 Ma BP interval in the stack has been constructed using records from the eastern Tropical Pacific. This region
 277 has been characterized by high upwelling rates and sedimentation rates in the past²⁰¹. While the CENOGRID composite has

278 a uniform resolution, higher sedimentation rates could affect the resolution of the original records and, therewith, even the
279 variability seen in lower-resolution sampling.

280 It follows from these remarks on Figs. 4(a,b) that variations in resolution of the data, which can arise from various factors
281 including measurement techniques and source region characteristics, can have a considerable effect on the frequency of detected
282 transitions. These factors can significantly impact the reliability of transition detection methods, thus highlighting the need for
283 caution when using individual records as proxies for global climate. While statistical indicators allow us to quantify jumps in
284 the data without any climatic context being provided, it is important to consider the limitations of such an approach, and to
285 supplement it with an independent understanding of the proxy data whenever possible. By doing so, we can better contextualize
286 and understand the implications of these jumps.

287 The Paraiso Cave record¹⁶⁵ from the eastern Amazon lowlands in Fig. 5 shows drier conditions during interglacials, with
288 abrupt transitions matching those that correspond to the DO events identified in the NGRIP ice core record. The Amazon record
289 is also in fairly good agreement with the nearby MD03-2621 marine sediment record. Notably, several of NGRIP's DO events
290 appear combined in both records, namely GI-5.2 and GI-5.1, as well as GI-10 and GI-9, which might indicate that a climate
291 change event over Greenland did not trigger a tipping event in the Amazon basin. Alternatively, the first merging may question
292 the separation of the classical GI-5 event²⁰² into two distinct events, 5.2 and 5.1.

293 The comparison of four records on the same time scale in Fig. 6 demonstrates that a signal of abrupt climate change is
294 detected when using the KS method with similar accuracy for different types of paleodata. The differences in the dates of the
295 transitions may be largely explained by the use of different age models in each of the records, with MD03-2621 fine-tuned to
296 the NGRIP chronology, and ODP893A fine-tuned to the GISP2 chronology, while the NGRIP and Paraiso Cave records were
297 independently dated. Notably, ODP893A data prior to GI-8 appear misaligned with the other three records. The chronology of
298 jumps in ODP893A indicates that the warm interval between 42.4 ka BP and 40.8 ka BP may correspond to an event spanning
299 GI-10 and GI-9, while the warm interval between 45.3 ka BP and 43.3 ka BP may correspond to GI-11.

300 It is important to keep in mind that age estimates of many paleoclimate records, including some of those discussed here,
301 are often not determined through independent methods, but rather are "tuned" or wiggle-matched to other records, such as
302 the global benthic $\delta^{18}\text{O}$ stack¹⁹⁷ or the NGRIP $\delta^{18}\text{O}$ record¹³¹. As the abrupt jumps in these records are themselves used as
303 tie-points, it is expected that the KS test would show a similarity in the timing of jumps in records that were tuned to the same
304 reference record. Therefore, any differences in the timing of transitions between these records should not be taken as indicative
305 of the chronology of events, but rather as a result of differences between the KS method and the transition detection method
306 used in the wiggle matching process. This fact should be taken into consideration when comparing records that have not been
307 independently dated.

308 In addition to the classical GI transitions, several additional jumps are identified in each of the marine and cave records.
309 These jumps may be the representative of local climate changes or, in some cases, be artifacts of sampling resolution or
310 measurement error. Stronger evidence for a local or regional event may be obtained when comparing two nearby records, like
311 the Paraiso Cave in the Amazon and the MD03-2621 marine record from the Cariaco Basin. In both records, the start of GI-5.2
312 is represented as two warming transitions, in contrast with the NGRIP and ODP893A records, where only one sharp transition
313 is present. Likewise, the end of GI-9 in the two tropical, South American records appears as two successive cooling events.
314 These results point to the potential of using the KS method to improve fine-tuning the synchronicity of two or more records,
315 when an independent dating method is not available.

316 The comparison in Fig. 7 of KS-detected transitions in marine core U1308⁹⁵ and in Lake Ohrid TIC¹³⁷ identifies the
317 transitions between individual glacials and interglacials. In the two records, the transitions are well identified, despite the
318 resolution of the two being different, and they offer a precise dating for the chronology of the past glacial cycles. The transitions
319 are overall in good agreement between the two records. Still, the warm events in Lake Ohrid are essentially atmospheric and
320 thus have often a shorter duration than in the marine record, while cooling transitions precede those in the deep ocean by several
321 thousand years. This could indicate that a significant time lag is present, either in ice sheet growth in response to atmospheric
322 cooling, or in the propagation of the cooling signal into the deep North Atlantic.

323 Furthermore, there are atmospheric interglacial episodes missing in the oceanic U1308 record. This mismatch between the
324 lake record¹³⁷ and the marine one⁹⁵ could be attributed to the fact that the KS test does sometimes find more transitions in
325 one record than in another one, even for the same type of proxy and within the same region. Such occurrences may be due to
326 the local environment, the sampling method, or some aspect of the KS method itself. When this is the case, it is important —
327 although not always feasible — to obtain additional records covering a similar time interval with a similar resolution, in order to
328 shed further light on the mismatch between the two original records. It should be noted that this study analyzed only one proxy
329 type from each location. A more comprehensive representation of past transitions could be achieved by investigating different
330 proxy records from the same core. For example, in contrast to the Rasmussen et al.¹³¹ study of the NGRIP record, which
331 analyzed both the $\delta^{18}\text{O}$ and Ca^{2+} proxies, this study only utilized $\delta^{18}\text{O}$ (Fig. 6a), which is a likely reason for not detecting the
332 GI-5.1 event.

333 Concluding remarks

334 The carefully selected, high-quality paleoproxy records in the open-source PaleoJump database¹⁸, <https://paleojump.github.io>,
335 have different temporal scales and a global spatial coverage; see again Fig. 1. These records provide an easily accessible
336 resource for research on potential tipping elements in Earth's climate. Still, major gaps in the marine sediment records exist
337 in the Southern Hemisphere, especially in the Indian and Pacific Oceans. Only sparse terrestrial data are available from the
338 high latitudes in both hemispheres, due to the recent glaciation. The only data from the African continent come from two East
339 African lake sediment records. Even though much information is at hand from the more than 100 sites listed in this paper, more
340 records are needed to fill geographical and temporal gaps, especially in the Southern Hemisphere.

341 The examples given in the paper on abrupt-transition identification demonstrate the usefulness of the records included
342 in PaleoJump for learning about potential tipping events in Earth's history and for comparing such events across different
343 locations around the world. The accessibility of such high-quality records is an invaluable resource for the climate modeling
344 community that requires comparing their results across a hierarchy of models^{183,203} with observations.

345 We also demonstrated the usefulness of the KS test¹⁹ for reconstructing the chronology of Earth's main climatic events. The
346 newly developed tool for automatic detection of abrupt transitions may be applied to different types of paleorecords, allowing
347 to objectively and robustly characterize the tipping phenomenon for climate subsystems already suspected of being subject
348 to tipping⁹, but also to identify previously unrecognized tipping elements in past climates. The observational descriptions
349 of tipping that can be obtained from PaleoJump using our KS methodology, combined with the application of Earth System
350 Models, can help improve the understanding of the bifurcation mechanisms of global and regional climate and identify possible
351 TPs for future climates.

352 Our results also indicate that paleorecord interpretations may vary, since the abrupt transitions identified in them will depend
353 on the time scale and type of variability that is investigated. For example, the KS method's parameters¹⁹ may be changed when
354 studying different proxy record resolutions, affecting the frequency and exact timing of the TPs that are identified.

355 The agreement in timing and pattern between jumps in distinct records can confirm the correctness of each record separately,
356 as well as of the inferences on climate variability drawn from these jumps. Specifically, the ability of the KS method to identify
357 matching small-scale transitions in different high-resolution records may be used to validate these transitions as being the result
358 of genuine global or regional climatic events, as opposed to just sampling errors. Furthermore, significant differences in records
359 that are, overall, in good agreement with each other may help decode the chronology of tipping events or an approximate range
360 for a tipping threshold. A fortiori, the differences in timing and pattern between jumps in distinct records that we also found
361 emphasize the importance of a consistent dating methodology.

362 In a potential second step, the transition detection tools presented here could be used for harmonizing and synchronizing
363 the records of the PaleoJump database, in a way that resembles the work conducted by several research teams in recent
364 years^{13,159,204–207}. Doing so would facilitate interpreting the abrupt changes in these records.

365 The broad spatial coverage of the PaleoJump database¹⁸, <https://paleojump.github.io>, with its records that vary in their
366 nature — ice, marine and land — as well as in their length and resolution, will facilitate research on tipping elements in
367 Earth's climate, including the polar ice sheets, the Atlantic Meridional Overturning Circulation, and the tropical rainforests and
368 monsoon systems. Furthermore, it will support establishing improved criteria on where and how to collect data for reliable
369 early warning signals of impending TPs.

370 Data availability

371 The datasets analyzed during the current study are available through Zenodo (<https://doi.org/10.5281/zenodo.6534031>)¹⁸ and
372 on the PaleoJump website, <https://paleojump.github.io>. The source code of the PaleoJump website can be found on GitHub at
373 <https://github.com/paleojump/paleojump>. The codes used for KS and RQA analyses are part of the TiPES statistical toolbox,
374 available on GitHub at https://github.com/paleojump/TiPES_statistical_toolbox.

375 References

- 376 1. Dansgaard, W. *et al.* A new Greenland deep ice core. *Science* **218**, 1273–1277 (1982).
- 377 2. Johnsen, S. *et al.* Irregular glacial interstadials recorded in a new Greenland ice core. *Nature* **359**, 311–313 (1992).
- 378 3. Grootes, P. M., Stuiver, M., White, J., Johnsen, S. & Jouzel, J. Comparison of oxygen isotope records from the GISP2
379 and GRIP Greenland ice cores. *Nature* **366**, 552–554 (1993).
- 380 4. Shackleton, N. J., Hall, M. A. & Vincent, E. Phase relationships between millennial-scale events 64,000–24,000 years
381 ago. *Paleoceanography* **15**, 565–569 (2000).

- 382 5. Genty, D. *et al.* Precise dating of Dansgaard–Oeschger climate oscillations in western Europe from stalagmite data.
383 *Nature* **421**, 833–837 (2003).
- 384 6. Ghil, M. & Childress, S. *Topics in Geophysical Fluid Dynamics: Atmospheric Dynamics, Dynamo Theory, and Climate*
385 *Dynamics* (Springer Science+Business Media, Berlin/Heidelberg, 1987). Reissued as an eBook in 2012.
- 386 7. Ghil, M. & Lucarini, V. The physics of climate variability and climate change. *Reviews of Modern Physics* **92**, 035002
387 (2020).
- 388 8. Pearce, F. *With Speed and Violence: Why Scientists Fear Tipping Points in Climate Change* (Beacon Press, 2007).
- 389 9. Lenton, T. M. *et al.* Tipping elements in the Earth’s climate system. *Proceedings of the National Academy of Sciences*
390 **105**, 1786–1793 (2008).
- 391 10. Scheffer, M. *et al.* Early-warning signals for critical transitions. *Nature* **461**, 53–59 (2009).
- 392 11. Sánchez Goñi, M. F. *et al.* The ACER pollen and charcoal database: a global resource to document vegetation and fire
393 response to abrupt climate changes during the last glacial period. *Earth System Science Data* **9**, 679–695 (2017).
- 394 12. Atsawawaranunt, K. *et al.* The SISAL database: a global resource to document oxygen and carbon isotope records from
395 speleothems. *Earth System Science Data* **10**, 1687–1713 (2018).
- 396 13. Jonkers, L. *et al.* Integrating palaeoclimate time series with rich metadata for uncertainty modelling: strategy and
397 documentation of the PalMod 130k marine palaeoclimate data synthesis. *Earth System Science Data* **12**, 1053–1081
398 (2020).
- 399 14. Mulitza, S. *et al.* World Atlas of late Quaternary Foraminiferal Oxygen and Carbon Isotope Ratios. *Earth System Science*
400 *Data* **14**, 2553–2611 (2022).
- 401 15. Judd, E. J. *et al.* The PhanSST global database of Phanerozoic sea surface temperature proxy data. *Scientific Data* **9**,
402 1–38 (2022).
- 403 16. Ghil, M. Hilbert problems for the geosciences in the 21st century. *Nonlinear Processes in Geophysics* **8**, 211–211 (2001).
- 404 17. Wunderling, N., Donges, J. F., Kurths, J. & Winkelmann, R. Interacting tipping elements increase risk of climate domino
405 effects under global warming. *Earth System Dynamics* **12**, 601–619 (2021).
- 406 18. Bagniewski, W., Rousseau, D.-D. & Ghil, M. Paleojump (2022). URL [https://doi.org/10.5281/zenodo.](https://doi.org/10.5281/zenodo.6534031)
407 [6534031](https://doi.org/10.5281/zenodo.6534031).
- 408 19. Bagniewski, W., Ghil, M. & Rousseau, D.-D. Automatic detection of abrupt transitions in paleoclimate records. *Chaos*
409 **31**, 113129 (2021).
- 410 20. Eckmann, J.-P., Kamphorst, S. O. & Ruelle, D. Recurrence plots of dynamical systems. *Europhysics Letters* **4**, 973–977
411 (1987).
- 412 21. Marwan, N., Romano, M. C., Thiel, M. & Kurths, J. Recurrence plots for the analysis of complex systems. *Physics*
413 *Reports* **438**, 237–329 (2007).
- 414 22. Thompson, L. G. *et al.* Tropical climate instability: The last glacial cycle from a Qinghai-Tibetan ice core. *Science* **276**,
415 1821–1825 (1997).
- 416 23. Westerhold, T. *et al.* An astronomically dated record of Earth’s climate and its predictability over the last 66 million years.
417 *Science* **369**, 1383–1387 (2020).
- 418 24. Sun, Y., Clemens, S. C., An, Z. & Yu, Z. Astronomical timescale and palaeoclimatic implication of stacked 3.6-myrr
419 monsoon records from the chinese loess plateau. *Quaternary Science Reviews* **25**, 33–48 (2006).
- 420 25. Boers, N., Goswami, B. & Ghil, M. A complete representation of uncertainties in layer-counted paleoclimatic archives.
421 *Climate of the Past* **13**, 1169–1180 (2017).
- 422 26. Goswami, B. *et al.* Abrupt transitions in time series with uncertainties. *Nature Communications* **9**, 1–10 (2018).
- 423 27. Blunier, T. & Brook, E. J. Timing of millennial-scale climate change in Antarctica and Greenland during the last glacial
424 period. *Science* **291**, 109–112 (2001).
- 425 28. Skinner, L. & Shackleton, N. An Atlantic lead over Pacific deep-water change across Termination I: implications for the
426 application of the marine isotope stage stratigraphy. *Quaternary Science Reviews* **24**, 571–580 (2005).
- 427 29. Shackleton, N. Oxygen isotope analyses and Pleistocene temperatures re-assessed. *Nature* **215**, 15–17 (1967).
- 428 30. McDermott, F. Palaeo-climate reconstruction from stable isotope variations in speleothems: a review. *Quaternary Science*
429 *Reviews* **23**, 901–918 (2004).

- 430 **31.** Bagniewski, W., Meissner, K. J., Menviel, L. & Brennan, C. E. Quantification of factors impacting seawater and calcite
431 $\delta^{18}\text{O}$ during Heinrich Stadials 1 and 4. *Paleoceanography* **30**, 895–911 (2015).
- 432 **32.** Allen, J. R. *et al.* Rapid environmental changes in southern Europe during the last glacial period. *Nature* **400**, 740–743
433 (1999).
- 434 **33.** Allen, J. R., Watts, W. A. & Huntley, B. Weichselian palynostratigraphy, palaeovegetation and palaeoenvironment; the
435 record from Lago Grande di Monticchio, southern Italy. *Quaternary International* **73**, 91–110 (2000).
- 436 **34.** Ampel, L., Wohlfarth, B., Risberg, J. & Veres, D. Paleolimnological response to millennial and centennial scale climate
437 variability during MIS 3 and 2 as suggested by the diatom record in Les Echets, France. *Quaternary Science Reviews* **27**,
438 1493–1504 (2008).
- 439 **35.** Arienzo, M. M. *et al.* Bahamian speleothem reveals temperature decrease associated with Heinrich stadials. *Earth and*
440 *Planetary Science Letters* **430**, 377–386 (2015).
- 441 **36.** Asmerom, Y., Polyak, V. J. & Burns, S. J. Variable winter moisture in the southwestern United States linked to rapid
442 glacial climate shifts. *Nature Geoscience* **3**, 114–117 (2010).
- 443 **37.** Bahr, A. *et al.* Oceanic heat pulses fueling moisture transport towards continental Europe across the mid-Pleistocene
444 transition. *Quaternary Science Reviews* **179**, 48–58 (2018).
- 445 **38.** Bar-Matthews, M., Ayalon, A., Gilmour, M., Matthews, A. & Hawkesworth, C. J. Sea–land oxygen isotopic relationships
446 from planktonic foraminifera and speleothems in the Eastern Mediterranean region and their implication for paleorainfall
447 during interglacial intervals. *Geochimica et Cosmochimica Acta* **67**, 3181–3199 (2003).
- 448 **39.** Barbante, C. *et al.* One-to-one coupling of glacial climate variability in Greenland and Antarctica. *Nature* **444**, 195–198
449 (2006).
- 450 **40.** Barker, S. *et al.* 800,000 years of abrupt climate variability. *Science* **334**, 347–351 (2011).
- 451 **41.** Barker, S. & Diz, P. Timing of the descent into the last Ice Age determined by the bipolar seesaw. *Paleoceanography* **29**,
452 489–507 (2014).
- 453 **42.** Barker, S. *et al.* Early interglacial legacy of deglacial climate instability. *Paleoceanography and Paleoclimatology* **34**,
454 1455–1475 (2019).
- 455 **43.** Baumgartner, M. *et al.* NGRIP CH 4 concentration from 120 to 10 kyr before present and its relation to a $\delta^{15}\text{N}$
456 temperature reconstruction from the same ice core. *Climate of the Past* **10**, 903–920 (2014).
- 457 **44.** Bazin, L. *et al.* An optimized multi-proxy, multi-site Antarctic ice and gas orbital chronology (AICC2012): 120–800 ka.
458 *Climate of the Past* **9**, 1715–1731 (2013).
- 459 **45.** Benson, L., Lund, S., Negrini, R., Linsley, B. & Zic, M. Response of north American Great basin lakes to Dansgaard–
460 Oeschger oscillations. *Quaternary Science Reviews* **22**, 2239–2251 (2003).
- 461 **46.** Beuscher, S. *et al.* End-member modelling as a tool for climate reconstruction—an Eastern Mediterranean case study.
462 *PLoS One* **12**, e0185136 (2017).
- 463 **47.** Boch, R. *et al.* NALPS: a precisely dated European climate record 120–60 ka. *Climate of the Past* **7**, 1247–1259 (2011).
- 464 **48.** Bolton, C. T. *et al.* North Atlantic midlatitude surface-circulation changes through the Plio-Pleistocene intensification of
465 Northern Hemisphere glaciation. *Paleoceanography and Paleoclimatology* **33**, 1186–1205 (2018).
- 466 **49.** Burns, S. J., Fleitmann, D., Matter, A., Kramers, J. & Al-Subbary, A. A. Indian Ocean climate and an absolute chronology
467 over Dansgaard/Oeschger events 9 to 13. *Science* **301**, 1365–1367 (2003).
- 468 **50.** Camuera, J. *et al.* Orbital-scale environmental and climatic changes recorded in a new 200,000-year-long multiproxy
469 sedimentary record from Padul, southern Iberian Peninsula. *Quaternary Science Reviews* **198**, 91–114 (2018).
- 470 **51.** Camuera, J. *et al.* Chronological control and centennial-scale climatic subdivisions of the Last Glacial Termination in the
471 western Mediterranean region. *Quaternary Science Reviews* **255**, 106814 (2021).
- 472 **52.** Camuera, J. *et al.* Past 200 kyr hydroclimate variability in the western mediterranean and its connection to the african
473 humid periods. *Scientific Reports* **12**, 1–13 (2022).
- 474 **53.** Carolin, S. A. *et al.* Varied response of western Pacific hydrology to climate forcings over the last glacial period. *Science*
475 **340**, 1564–1566 (2013).
- 476 **54.** Cheng, H. *et al.* The climatic cyclicity in semiarid-arid central Asia over the past 500,000 years. *Geophysical Research*
477 *Letters* **39** (2012).

- 478 55. Cheng, H. *et al.* The Asian monsoon over the past 640,000 years and ice age terminations. *Nature* **534**, 640–646 (2016).
- 479 56. Cheng, H. *et al.* Climate variations of Central Asia on orbital to millennial timescales. *Scientific Reports* **6**, 1–11 (2016).
- 480 57. Clemens, S. *et al.* Precession-band variance missing from East Asian monsoon runoff. *Nature Communications* **9**, 1–12
481 (2018).
- 482 58. Clemens, S. C. *et al.* Remote and local drivers of Pleistocene South Asian summer monsoon precipitation: A test for
483 future predictions. *Science Advances* **7**, eabg3848 (2021).
- 484 59. Cruz, F. W. *et al.* Insolation-driven changes in atmospheric circulation over the past 116,000 years in subtropical Brazil.
485 *Nature* **434**, 63–66 (2005).
- 486 60. Davtian, N., Bard, E., Darfeuil, S., Ménot, G. & Rostek, F. The Novel Hydroxylated Tetraether Index RI-OH' as a Sea
487 Surface Temperature Proxy for the 160-45 ka BP Period Off the Iberian Margin. *Paleoceanography and Paleoclimatology*
488 **36**, e2020PA004077 (2021).
- 489 61. de Abreu, L., Shackleton, N. J., Schönfeld, J., Hall, M. & Chapman, M. Millennial-scale oceanic climate variability off
490 the Western Iberian margin during the last two glacial periods. *Marine Geology* **196**, 1–20 (2003).
- 491 62. De Deckker, P. *et al.* Climatic evolution in the Australian region over the last 94 ka-spanning human occupancy-, and
492 unveiling the Last Glacial Maximum. *Quaternary Science Reviews* **249**, 106593 (2020).
- 493 63. Denniston, R. F. *et al.* North Atlantic forcing of millennial-scale Indo-Australian monsoon dynamics during the Last
494 Glacial period. *Quaternary Science Reviews* **72**, 159–168 (2013).
- 495 64. Deplazes, G. *et al.* Links between tropical rainfall and North Atlantic climate during the last glacial period. *Nature*
496 *Geoscience* **6**, 213–217 (2013).
- 497 65. Deplazes, G. *et al.* Weakening and strengthening of the Indian monsoon during Heinrich events and Dansgaard-Oeschger
498 oscillations. *Paleoceanography* **29**, 99–114 (2014).
- 499 66. De Pol-Holz, R. *et al.* Late Quaternary variability of sedimentary nitrogen isotopes in the eastern South Pacific Ocean.
500 *Paleoceanography* **22** (2007).
- 501 67. Dickson, A. J., Austin, W. E., Hall, I. R., Maslin, M. A. & Kucera, M. Centennial-scale evolution of Dansgaard-Oeschger
502 events in the northeast Atlantic Ocean between 39.5 and 56.5 ka BP. *Paleoceanography* **23** (2008).
- 503 68. Ding, Z. L. *et al.* Stacked 2.6-Ma grain size record from the Chinese loess based on five sections and correlation with the
504 deep-sea $\delta^{18}\text{O}$ record. *Paleoceanography* **17**, 5–1 (2002).
- 505 69. Dokken, T. M. & Jansen, E. Rapid changes in the mechanism of ocean convection during the last glacial period. *Nature*
506 **401**, 458–461 (1999).
- 507 70. Donders, T. *et al.* 1.36 million years of Mediterranean forest refugium dynamics in response to glacial–interglacial cycle
508 strength. *Proceedings of the National Academy of Sciences* **118** (2021).
- 509 71. Ehrmann, W. & Schmiedl, G. Nature and dynamics of North African humid and dry periods during the last 200,000 years
510 documented in the clay fraction of Eastern Mediterranean deep-sea sediments. *Quaternary Science Reviews* **260**, 106925
511 (2021).
- 512 72. Elderfield, H. *et al.* Evolution of ocean temperature and ice volume through the mid-Pleistocene climate transition.
513 *Science* **337**, 704–709 (2012).
- 514 73. Erhardt, T. *et al.* Decadal-scale progression of the onset of Dansgaard–Oeschger warming events. *Climate of the Past* **15**,
515 811–825 (2019).
- 516 74. Extier, T. *et al.* On the use of $\delta^{18}\text{O}_{\text{atm}}$ for ice core dating. *Quaternary Science Reviews* **185**, 244–257 (2018).
- 517 75. Eynaud, F. *et al.* Position of the Polar Front along the western Iberian margin during key cold episodes of the last 45 ka.
518 *Geochemistry, Geophysics, Geosystems* **10** (2009).
- 519 76. Fleitmann, D. *et al.* Timing and climatic impact of Greenland interstadials recorded in stalagmites from northern Turkey.
520 *Geophysical Research Letters* **36** (2009).
- 521 77. Follieri, M., Magri, D. & Sadori, L. Pollen stratigraphical synthesis from Valle di Castiglione (Roma). *Quaternary*
522 *International* **3**, 81–84 (1989).
- 523 78. Francke, A. *et al.* Sedimentological processes and environmental variability at Lake Ohrid (Macedonia, Albania) between
524 637 ka and the present. *Biogeosciences* **13**, 1179–1196 (2016).

- 525 **79.** Fritz, S. C. *et al.* Quaternary glaciation and hydrologic variation in the South American tropics as reconstructed from the
526 Lake Titicaca drilling project. *Quaternary Research* **68**, 410–420 (2007).
- 527 **80.** Fritz, S. C., Baker, P., Ekdahl, E., Seltzer, G. & Stevens, L. Millennial-scale climate variability during the Last Glacial
528 period in the tropical Andes. *Quaternary Science Reviews* **29**, 1017–1024 (2010).
- 529 **81.** Genty, D. *et al.* Isotopic characterization of rapid climatic events during OIS3 and OIS4 in Villars Cave stalagmites
530 (SW-France) and correlation with Atlantic and Mediterranean pollen records. *Quaternary Science Reviews* **29**, 2799–2820
531 (2010).
- 532 **82.** Gkinis, V. *et al.* A 120,000-year long climate record from a NW-Greenland deep ice core at ultra-high resolution. *Scientific*
533 *Data* **8**, 1–9 (2021).
- 534 **83.** Gottschalk, J., Skinner, L. C. & Waelbroeck, C. Contribution of seasonal sub-Antarctic surface water variability to
535 millennial-scale changes in atmospheric CO₂ over the last deglaciation and Marine Isotope Stage 3. *Earth and Planetary*
536 *Science Letters* **411**, 87–99 (2015).
- 537 **84.** Grimm, E. C. *et al.* Evidence for warm wet Heinrich events in Florida. *Quaternary Science Reviews* **25**, 2197–2211
538 (2006).
- 539 **85.** Hao, Q. *et al.* Delayed build-up of Arctic ice sheets during 400,000-year minima in insolation variability. *Nature* **490**,
540 393–396 (2012).
- 541 **86.** Harada, N. *et al.* Rapid fluctuation of alkenone temperature in the southwestern Okhotsk Sea during the past 120 ky.
542 *Global and Planetary Change* **53**, 29–46 (2006).
- 543 **87.** Hendy, I. L. & Kennett, J. P. Latest Quaternary North Pacific surface-water responses imply atmosphere-driven climate
544 instability. *Geology* **27**, 291–294 (1999).
- 545 **88.** Hendy, I. L., Kennett, J. P., Roark, E. & Ingram, B. L. Apparent synchronicity of submillennial scale climate events
546 between Greenland and Santa Barbara Basin, California from 30–10 ka. *Quaternary Science Reviews* **21**, 1167–1184
547 (2002).
- 548 **89.** Hendy, I. L. & Kennett, J. P. Tropical forcing of North Pacific intermediate water distribution during Late Quaternary
549 rapid climate change? *Quaternary Science Reviews* **22**, 673–689 (2003).
- 550 **90.** Hodell, D. A., Venz, K. A., Charles, C. D. & Ninnemann, U. S. Pleistocene vertical carbon isotope and carbonate
551 gradients in the South Atlantic sector of the Southern Ocean. *Geochemistry, Geophysics, Geosystems* **4**, 1–19 (2003).
- 552 **91.** Hodell, D. A., Channell, J. E., Curtis, J. H., Romero, O. E. & Röhl, U. Onset of “Hudson Strait” Heinrich events in the
553 eastern North Atlantic at the end of the middle Pleistocene transition (~640 ka)? *Paleoceanography* **23** (2008).
- 554 **92.** Hodell, D. A., Evans, H. F., Channell, J. E. & Curtis, J. H. Phase relationships of North Atlantic ice-rafted debris and
555 surface-deep climate proxies during the last glacial period. *Quaternary Science Reviews* **29**, 3875–3886 (2010).
- 556 **93.** Hodell, D. *et al.* Response of Iberian Margin sediments to orbital and suborbital forcing over the past 420 ka. *Paleo-*
557 *ceanography* **28**, 185–199 (2013).
- 558 **94.** Hodell, D. *et al.* A reference time scale for Site U1385 (Shackleton Site) on the SW Iberian Margin. *Global and Planetary*
559 *Change* **133**, 49–64 (2015).
- 560 **95.** Hodell, D. A. & Channell, J. E. Mode transitions in Northern Hemisphere glaciation: co-evolution of millennial and
561 orbital variability in Quaternary climate. *Climate of the Past* **12**, 1805–1828 (2016).
- 562 **96.** Huntley, B., Watts, W., Allen, J. & Zolitschka, B. Palaeoclimate, chronology and vegetation history of the Weichselian
563 Lateglacial: comparative analysis of data from three cores at Lago Grande di Monticchio, southern Italy. *Quaternary*
564 *Science Reviews* **18**, 945–960 (1999).
- 565 **97.** Johnson, T. C. *et al.* A progressively wetter climate in southern East Africa over the past 1.3 million years. *Nature* **537**,
566 220–224 (2016).
- 567 **98.** Jouzel, J. *et al.* Orbital and millennial Antarctic climate variability over the past 800,000 years. *Science* **317**, 793–796
568 (2007).
- 569 **99.** Jung, S. J., Kroon, D., Ganssen, G., Peeters, F. & Ganeshram, R. Enhanced Arabian Sea intermediate water flow during
570 glacial North Atlantic cold phases. *Earth and Planetary Science Letters* **280**, 220–228 (2009).
- 571 **100.** Kanner, L. C., Burns, S. J., Cheng, H. & Edwards, R. L. High-latitude forcing of the South American summer monsoon
572 during the last glacial. *Science* **335**, 570–573 (2012).

- 573 **101.** Kathayat, G. *et al.* Indian monsoon variability on millennial-orbital timescales. *Scientific Reports* **6**, 1–7 (2016).
- 574 **102.** Kelly, M. J. *et al.* High resolution characterization of the Asian Monsoon between 146,000 and 99,000 years BP from
575 Dongge Cave, China and global correlation of events surrounding Termination II. *Palaeogeography, Palaeoclimatology,*
576 *Palaeoecology* **236**, 20–38 (2006).
- 577 **103.** Lachniet, M. S. *et al.* Late Quaternary moisture export across Central America and to Greenland: evidence for tropical
578 rainfall variability from Costa Rican stalagmites. *Quaternary Science Reviews* **28**, 3348–3360 (2009).
- 579 **104.** Lachniet, M. S., Denniston, R. F., Asmerom, Y. & Polyak, V. J. Orbital control of western North America atmospheric
580 circulation and climate over two glacial cycles. *Nature Communications* **5**, 1–8 (2014).
- 581 **105.** Lambert, F. *et al.* Dust-climate couplings over the past 800,000 years from the EPICA Dome C ice core. *Nature* **452**,
582 616–619 (2008).
- 583 **106.** Lambert, F., Bigler, M., Steffensen, J. P., Hutterli, M. & Fischer, H. Centennial mineral dust variability in high-resolution
584 ice core data from Dome C, Antarctica. *Climate of the Past* **8**, 609–623 (2012).
- 585 **107.** Lauterbach, S. *et al.* An ~130 kyr record of surface water temperature and $\delta^{18}\text{O}$ from the northern Bay of Bengal:
586 Investigating the linkage between Heinrich events and Weak Monsoon Intervals in Asia. *Paleoceanography and*
587 *Paleoclimatology* **35**, e2019PA003646 (2020).
- 588 **108.** Lea, D. W. *et al.* Paleoclimate history of Galápagos surface waters over the last 135,000 yr. *Quaternary Science Reviews*
589 **25**, 1152–1167 (2006).
- 590 **109.** Louergue, L. *et al.* Orbital and millennial-scale features of atmospheric CH₄ over the past 800,000 years. *Nature* **453**,
591 383–386 (2008).
- 592 **110.** Lüthi, D. *et al.* High-resolution carbon dioxide concentration record 650,000–800,000 years before present. *Nature* **453**,
593 379–382 (2008).
- 594 **111.** Martrat, B. *et al.* Four climate cycles of recurring deep and surface water destabilizations on the Iberian margin. *Science*
595 **317**, 502–507 (2007).
- 596 **112.** Melles, M. *et al.* 2.8 million years of Arctic climate change from Lake El’gygytgyn, NE Russia. *Science* **337**, 315–320
597 (2012).
- 598 **113.** Meyer-Jacob, C. *et al.* Biogeochemical variability during the past 3.6 million years recorded by FTIR spectroscopy in the
599 sediment record of Lake El’gygytgyn, Far East Russian Arctic. *Climate of the Past* **10**, 209–220 (2014).
- 600 **114.** Miebach, A., Stolzenberger, S., Wacker, L., Hense, A. & Litt, T. A new Dead Sea pollen record reveals the last glacial
601 paleoenvironment of the southern Levant. *Quaternary Science Reviews* **214**, 98–116 (2019).
- 602 **115.** Mohtadi, M. *et al.* North Atlantic forcing of tropical Indian Ocean climate. *Nature* **509**, 76–80 (2014).
- 603 **116.** Moine, O. *et al.* The impact of Last Glacial climate variability in west-European loess revealed by radiocarbon dating of
604 fossil earthworm granules. *Proceedings of the National Academy of Sciences* **114**, 6209–6214 (2017).
- 605 **117.** Mosblech, N. A. *et al.* North Atlantic forcing of Amazonian precipitation during the last ice age. *Nature Geoscience* **5**,
606 817–820 (2012).
- 607 **118.** Moseley, G. E. *et al.* NALPS19: sub-orbital-scale climate variability recorded in northern Alpine speleothems during the
608 last glacial period. *Climate of the Past* **16**, 29–50 (2020).
- 609 **119.** Müller, U. C., Pross, J. & Bibus, E. Vegetation response to rapid climate change in Central Europe during the past 140,000
610 yr based on evidence from the Füramoos pollen record. *Quaternary Research* **59**, 235–245 (2003).
- 611 **120.** Naafs, B., Hefter, J. & Stein, R. Millennial-scale ice rafting events and Hudson Strait Heinrich (-like) Events during the
612 late Pliocene and Pleistocene: a review. *Quaternary Science Reviews* **80**, 1–28 (2013).
- 613 **121.** Naafs, B. D. A., Voelker, A., Karas, C., Andersen, N. & Sierro, F. Repeated near-collapse of the Pliocene sea surface
614 temperature gradient in the North Atlantic. *Paleoceanography and Paleoclimatology* **35**, e2020PA003905 (2020).
- 615 **122.** Naughton, F. *et al.* Wet to dry climatic trend in north-western Iberia within Heinrich events. *Earth and Planetary Science*
616 *Letters* **284**, 329–342 (2009).
- 617 **123.** Nürnberg, D., Ziegler, M., Karas, C., Tiedemann, R. & Schmidt, M. W. Interacting Loop Current variability and
618 Mississippi River discharge over the past 400 kyr. *Earth and Planetary Science Letters* **272**, 278–289 (2008).
- 619 **124.** Pahnke, K., Zahn, R., Elderfield, H. & Schulz, M. 340,000-year centennial-scale marine record of Southern Hemisphere
620 climatic oscillation. *Science* **301**, 948–952 (2003).

- 621 **125.** Petit, J.-R. *et al.* Climate and atmospheric history of the past 420,000 years from the Vostok ice core, Antarctica. *Nature*
622 **399**, 429–436 (1999).
- 623 **126.** Pichevin, L., Bard, E., Martinez, P. & Billy, I. Evidence of ventilation changes in the Arabian Sea during the late
624 Quaternary: Implication for denitrification and nitrous oxide emission. *Global Biogeochemical Cycles* **21** (2007).
- 625 **127.** Pickarski, N. & Litt, T. A new high-resolution pollen sequence at Lake Van, Turkey: insights into penultimate interglacial–
626 glacial climate change on vegetation history. *Climate of the Past* **13**, 689–710 (2017).
- 627 **128.** Prokopenko, A. A., Hinnov, L. A., Williams, D. F. & Kuzmin, M. I. Orbital forcing of continental climate during the
628 Pleistocene: a complete astronomically tuned climatic record from Lake Baikal, SE Siberia. *Quaternary Science Reviews*
629 **25**, 3431–3457 (2006).
- 630 **129.** Rampen, S. W. *et al.* Long chain 1, 13-and 1, 15-diols as a potential proxy for palaeotemperature reconstruction.
631 *Geochimica et Cosmochimica Acta* **84**, 204–216 (2012).
- 632 **130.** Rasmussen, S. O. *et al.* A first chronology for the North Greenland Eemian Ice Drilling (NEEM) ice core. *Climate of the*
633 *Past* **9**, 2713–2730 (2013).
- 634 **131.** Rasmussen, S. O. *et al.* A stratigraphic framework for abrupt climatic changes during the Last Glacial period based on
635 three synchronized Greenland ice-core records: refining and extending the INTIMATE event stratigraphy. *Quaternary*
636 *Science Reviews* **106**, 14–28 (2014).
- 637 **132.** Reille, M. & De Beaulieu, J. Pollen analysis of a long upper Pleistocene continental sequence in a Velay maar (Massif
638 Central, France). *Palaeogeography, Palaeoclimatology, Palaeoecology* **80**, 35–48 (1990).
- 639 **133.** Rickaby, R. E. M. & Elderfield, H. Planktonic foraminiferal Cd/Ca: paleonutrients or paleotemperature? *Paleoceanogra-*
640 *phy* **14**, 293–303 (1999).
- 641 **134.** Riveiros, N. V. *et al.* Response of South Atlantic deep waters to deglacial warming during Terminations V and I. *Earth*
642 *and Planetary Science Letters* **298**, 323–333 (2010).
- 643 **135.** Rosenthal, Y., Oppo, D. W. & Linsley, B. K. The amplitude and phasing of climate change during the last deglaciation in
644 the Sulu Sea, western equatorial Pacific. *Geophysical Research Letters* **30** (2003).
- 645 **136.** Rousseau, D.-D. *et al.* (MIS3 & 2) millennial oscillations in Greenland dust and Eurasian aeolian records—A paleosol
646 perspective. *Quaternary Science Reviews* **169**, 99–113 (2017).
- 647 **137.** Sadori, L. *et al.* Pollen-based paleoenvironmental and paleoclimatic change at Lake Ohrid (south-eastern Europe) during
648 the past 500 ka. *Biogeosciences* **13**, 1423–1437 (2016).
- 649 **138.** Saikku, R., Stott, L. & Thunell, R. A bi-polar signal recorded in the western tropical Pacific: Northern and Southern
650 Hemisphere climate records from the Pacific warm pool during the last Ice Age. *Quaternary Science Reviews* **28**,
651 2374–2385 (2009).
- 652 **139.** Salgueiro, E. *et al.* Past circulation along the western Iberian margin: a time slice vision from the Last Glacial to the
653 Holocene. *Quaternary Science Reviews* **106**, 316–329 (2014).
- 654 **140.** Schulz, H., von Rad, U. & Erlenkeuser, H. Correlation between Arabian Sea and Greenland climate oscillations of the
655 past 110,000 years. *Nature* **393**, 54–57 (1998).
- 656 **141.** Seelos, K., Sirocko, F. & Dietrich, S. A continuous high-resolution dust record for the reconstruction of wind systems in
657 central Europe (Eifel, Western Germany) over the past 133 ka. *Geophysical Research Letters* **36** (2009).
- 658 **142.** Stott, L., Poulsen, C., Lund, S. & Thunell, R. Super ENSO and global climate oscillations at millennial time scales.
659 *Science* **297**, 222–226 (2002).
- 660 **143.** Strikis, N. M. *et al.* South American monsoon response to iceberg discharge in the North Atlantic. *Proceedings of the*
661 *National Academy of Sciences* **115**, 3788–3793 (2018).
- 662 **144.** Sun, Y., Wang, X., Liu, Q. & Clemens, S. C. Impacts of post-depositional processes on rapid monsoon signals recorded
663 by the last glacial loess deposits of northern China. *Earth and Planetary Science Letters* **289**, 171–179 (2010).
- 664 **145.** Sun, Y. *et al.* Influence of Atlantic meridional overturning circulation on the East Asian winter monsoon. *Nature*
665 *Geoscience* **5**, 46–49 (2012).
- 666 **146.** Sun, Y. *et al.* Astronomical and glacial forcing of East Asian summer monsoon variability. *Quaternary Science Reviews*
667 **115**, 132–142 (2015).
- 668 **147.** Sun, Y. *et al.* High-sedimentation-rate loess records: A new window into understanding orbital-and millennial-scale
669 monsoon variability. *Earth-Science Reviews* **220**, 103731 (2021).

- 670 **148.** Tierney, J. E. *et al.* Northern hemisphere controls on tropical southeast African climate during the past 60,000 years.
671 *Science* **322**, 252–255 (2008).
- 672 **149.** Tzedakis, P. *et al.* Ecological thresholds and patterns of millennial-scale climate variability: The response of vegetation in
673 Greece during the last glacial period. *Geology* **32**, 109–112 (2004).
- 674 **150.** Tzedakis, P., Hooghiemstra, H. & Pälike, H. The last 1.35 million years at Tenaghi Philippon: revised chronostratigraphy
675 and long-term vegetation trends. *Quaternary Science Reviews* **25**, 3416–3430 (2006).
- 676 **151.** Uemura, R. *et al.* Asynchrony between Antarctic temperature and CO₂ associated with obliquity over the past 720,000
677 years. *Nature Communications* **9**, 1–11 (2018).
- 678 **152.** Újvári, G. *et al.* AMS 14C and OSL/IRSL dating of the Dunaszekcső loess sequence (Hungary): chronology for 20 to
679 150 ka and implications for establishing reliable age–depth models for the last 40 ka. *Quaternary Science Reviews* **106**,
680 140–154 (2014).
- 681 **153.** Ünal-İmer, E. *et al.* An 80 kyr-long continuous speleothem record from Dim Cave, SW Turkey with paleoclimatic
682 implications for the Eastern Mediterranean. *Scientific Reports* **5**, 1–11 (2015).
- 683 **154.** Vallelonga, P. *et al.* Iron fluxes to Talos Dome, Antarctica, over the past 200 kyr. *Climate of the Past* **9**, 597–604 (2013).
- 684 **155.** Van Kreveld, S. *et al.* Potential links between surging ice sheets, circulation changes, and the Dansgaard-Oeschger cycles
685 in the Irminger Sea, 60–18 kyr. *Paleoceanography* **15**, 425–442 (2000).
- 686 **156.** Veres, D. *et al.* Climate-driven changes in lake conditions during late MIS 3 and MIS 2: a high-resolution geochemical
687 record from Les Echets, France. *Boreas* **38**, 230–243 (2009).
- 688 **157.** Voelker, A. H. *et al.* Mediterranean outflow strengthening during northern hemisphere coolings: a salt source for the
689 glacial Atlantic? *Earth and Planetary Science Letters* **245**, 39–55 (2006).
- 690 **158.** Voelker, A. H. & Abreu, L. d. A review of abrupt climate change events in the Northeastern Atlantic Ocean (Iberian
691 Margin): latitudinal, longitudinal and vertical gradients. *AGU Geophysical Monograph* (2010).
- 692 **159.** Waelbroeck, C. *et al.* Consistently dated Atlantic sediment cores over the last 40 thousand years. *Scientific Data* **6**, 1–12
693 (2019).
- 694 **160.** Wagner, J. D. *et al.* Moisture variability in the southwestern United States linked to abrupt glacial climate change. *Nature*
695 *Geoscience* **3**, 110–113 (2010).
- 696 **161.** Wagner, B. *et al.* Mediterranean winter rainfall in phase with African monsoons during the past 1.36 million years. *Nature*
697 **573**, 256–260 (2019).
- 698 **162.** WAIS Divide Project Members. Precise inter-polar phasing of abrupt climate change during the last ice age. *Nature* **520**,
699 661–665 (2015).
- 700 **163.** Wang, Y.-J. *et al.* A high-resolution absolute-dated late Pleistocene monsoon record from Hulu Cave, China. *Science* **294**,
701 2345–2348 (2001).
- 702 **164.** Wang, Y. *et al.* Millennial-and orbital-scale changes in the East Asian monsoon over the past 224,000 years. *Nature* **451**,
703 1090–1093 (2008).
- 704 **165.** Wang, X. *et al.* Hydroclimate changes across the Amazon lowlands over the past 45,000 years. *Nature* **541**, 204–207
705 (2017).
- 706 **166.** Weijers, J. W., Schouten, S., Schefuß, E., Schneider, R. R. & Damste, J. S. S. Disentangling marine, soil and plant organic
707 carbon contributions to continental margin sediments: a multi-proxy approach in a 20,000 year sediment record from the
708 Congo deep-sea fan. *Geochimica et Cosmochimica Acta* **73**, 119–132 (2009).
- 709 **167.** Weldeab, S., Emeis, K.-C., Hemleben, C., Schmiedl, G. & Schulz, H. Spatial productivity variations during formation
710 of sapropels S5 and S6 in the Mediterranean Sea: evidence from Ba contents. *Palaeogeography, Palaeoclimatology,*
711 *Palaeoecology* **191**, 169–190 (2003).
- 712 **168.** Weldeab, S., Lea, D. W., Schneider, R. R. & Andersen, N. 155,000 years of West African monsoon and ocean thermal
713 evolution. *Science* **316**, 1303–1307 (2007).
- 714 **169.** Whittaker, T. E., Hendy, C. H. & Hellstrom, J. C. Abrupt millennial-scale changes in intensity of Southern Hemisphere
715 westerly winds during marine isotope stages 2–4. *Geology* **39**, 455–458 (2011).
- 716 **170.** Yang, S. & Ding, Z. A 249 kyr stack of eight loess grain size records from northern China documenting millennial-scale
717 climate variability. *Geochemistry, Geophysics, Geosystems* **15**, 798–814 (2014).

- 718 **171.** Zariess, M. & Mackensen, A. The tropical rainbelt and productivity changes off northwest Africa: A 31,000-year
719 high-resolution record. *Marine Micropaleontology* **76**, 76–91 (2010).
- 720 **172.** Zariess, M. *et al.* Bipolar seesaw in the northeastern tropical atlantic during heinrich stadials. *Geophysical Research*
721 *Letters* **38** (2011).
- 722 **173.** Zhao, M., Beveridge, N., Shackleton, N., Sarnthein, M. & Eglinton, G. Molecular stratigraphy of cores off northwest
723 Africa: Sea surface temperature history over the last 80 ka. *Paleoceanography* **10**, 661–675 (1995).
- 724 **174.** Ziegler, M., Diz, P., Hall, I. R. & Zahn, R. Millennial-scale changes in atmospheric CO₂ levels linked to the Southern
725 Ocean carbon isotope gradient and dust flux. *Nature Geoscience* **6**, 457–461 (2013).
- 726 **175.** Massey Jr, F. J. The Kolmogorov-Smirnov test for goodness of fit. *Journal of the American Statistical Association* **46**,
727 68–78 (1951).
- 728 **176.** Conover, W. J. *Practical Nonparametric Statistics* (John Wiley & Sons, 1999).
- 729 **177.** Fawcett, T. An introduction to ROC analysis. *Pattern Recognition Letters* **27**, 861–874 (2006).
- 730 **178.** Hastie, T., Tibshirani, R. & Friedman, J. *The Elements of Statistical Learning: Data Mining, Inference, and Prediction*
731 (Springer Science & Business Media, 2009).
- 732 **179.** Marwan, N., Schinkel, S. & Kurths, J. Recurrence plots 25 years later—Gaining confidence in dynamical transitions.
733 *Europhysics Letters* **101**, 20007 (2013).
- 734 **180.** Ghil, M., Chekroun, M. D. & Simonnet, E. Climate dynamics and fluid mechanics: natural variability and related
735 uncertainties. *Physica D: Nonlinear Phenomena* **237**, 2111–2126 (2008).
- 736 **181.** Chekroun, M. D., Simonnet, E. & Ghil, M. Stochastic climate dynamics: random attractors and time-dependent invariant
737 measures. *Physica D: Nonlinear Phenomena* **240**, 1685–1700 (2011).
- 738 **182.** Bódai, T. & Tél, T. Annual variability in a conceptual climate model: Snapshot attractors, hysteresis in extreme events,
739 and climate sensitivity. *Chaos* **22**, 023110 (2012).
- 740 **183.** Ghil, M. A century of nonlinearity in the geosciences. *Earth and Space Science* **6**, 1007–1042 (2019).
- 741 **184.** Riechers, K., Mitsui, T., Boers, N. & Ghil, M. Orbital insolation variations, intrinsic climate variability, and Quaternary
742 glaciations. *Climate of the Past* **18**, 863–893 (2022).
- 743 **185.** Bradley, R. S. & Diaz, H. F. Late Quaternary Abrupt Climate Change in the Tropics and Sub-Tropics: The Continental
744 Signal of Tropical Hydroclimatic Events (THEs). *Reviews of Geophysics* **59**, e2020RG000732 (2021).
- 745 **186.** Zachos, J., Pagani, M., Sloan, L., Thomas, E. & Billups, K. Trends, rhythms, and aberrations in global climate 65 Ma to
746 present. *Science* **292**, 686–693 (2001).
- 747 **187.** Coxall, H. K., Wilson, P. A., Pälike, H., Lear, C. H. & Backman, J. Rapid stepwise onset of Antarctic glaciation and
748 deeper calcite compensation in the Pacific Ocean. *Nature* **433**, 53–57 (2005).
- 749 **188.** Rousseau, D.-D., Bagniewski, W. & Lucarini, V. A Punctuated Equilibrium Analysis of the Climate Evolution of
750 Cenozoic: Hierarchy of Abrupt Transitions. *Preprint available at Research Square* doi.org/10.21203/rs.3.rs-2359196/v1
751 (2022).
- 752 **189.** Miller, K. G., Fairbanks, R. G. & Mountain, G. S. Tertiary oxygen isotope synthesis, sea level history, and continental
753 margin erosion. *Paleoceanography* **2**, 1–19 (1987).
- 754 **190.** Flower, B. P. & Kennett, J. P. The middle Miocene climatic transition: East Antarctic ice sheet development, deep ocean
755 circulation and global carbon cycling. *Palaeogeography, Palaeoclimatology, Palaeoecology* **108**, 537–555 (1994).
- 756 **191.** Miller, K. *et al.* Cenozoic sea-level and cryospheric evolution from deep-sea geochemical and continental margin records.
757 *Science Advances* **6**, 1346 (2020).
- 758 **192.** Rohling, E. *et al.* Sea level and deepsea temperature reconstructions suggest quasi-stable states and critical transitions
759 over the past 40 million years. *Science Advances* **7**, 5326 (2021).
- 760 **193.** Emiliani, C. & Geiss, J. On glaciations and their causes. *Geologische Rundschau* **46**, 576–601 (1959).
- 761 **194.** Boers, N., Marwan, N., Barbosa, H. M. J. & Kurths, J. A deforestation-induced tipping point for the South American
762 monsoon system. *Scientific Reports* **7** (2017).
- 763 **195.** Ruddiman, W. F. North Atlantic ice-rafting: a major change at 75,000 years before the present. *Science* **196**, 1208–1211
764 (1977).

- 765 **196.** Rousseau, D.-D., Bagniewski, W. & Ghil, M. Abrupt climate changes and the astronomical theory: are they related?
766 *Climate of the Past* **18**, 249–271 (2022).
- 767 **197.** Lisiecki, L. E. & Raymo, M. E. A Pliocene-Pleistocene stack of 57 globally distributed benthic $\delta^{18}\text{O}$ records. *Paleo-*
768 *ceanography* **20** (2005).
- 769 **198.** Miller, K. G., Wright, J. D. & Fairbanks, R. G. Unlocking the ice house: Oligocene-Miocene oxygen isotopes, eustasy,
770 and margin erosion. *Journal of Geophysical Research: Solid Earth* **96**, 6829–6848 (1991).
- 771 **199.** Boulila, S. *et al.* On the origin of Cenozoic and Mesozoic “third-order” eustatic sequences. *Earth-Science Reviews* **109**,
772 94–112 (2011).
- 773 **200.** Shackleton, N. J., Hall, M. A., Raffi, I., Tauxe, L. & Zachos, J. Astronomical calibration age for the Oligocene-Miocene
774 boundary. *Geology* **28**, 447–450 (2000).
- 775 **201.** Pinero, E., Marquardt, M., Hensen, C., Haeckel, M. & Wallmann, K. Estimation of the global inventory of methane
776 hydrates in marine sediments using transfer functions. *Biogeosciences* **10**, 959–975 (2013).
- 777 **202.** Dansgaard, W. *et al.* Evidence for general instability of past climate from a 250-kyr ice-core record. *Nature* **364**, 218–220
778 (1993).
- 779 **203.** Schneider, S. H. & Dickinson, R. E. Climate modeling. *Reviews of Geophysics* **12**, 447–493 (1974).
- 780 **204.** Buizert, C. *et al.* Abrupt ice-age shifts in southern westerly winds and Antarctic climate forced from the north. *Nature*
781 **563**, 681–685 (2018).
- 782 **205.** Adolphi, F. *et al.* Connecting the Greenland ice-core and U/Th timescales via cosmogenic radionuclides: testing the
783 synchronicity of Dansgaard–Oeschger events. *Climate of the Past* **14**, 1755–1781 (2018).
- 784 **206.** Comas-Bru, L. *et al.* SISALv2: a comprehensive speleothem isotope database with multiple age–depth models. *Earth*
785 *System Science Data* **12**, 2579–2606 (2020).
- 786 **207.** Lee, T., Rand, D., Lisiecki, L. E., Gebbie, G. & Lawrence, C. E. Bayesian age models and stacks: Combining age
787 inferences from radiocarbon and benthic $\delta^{18}\text{O}$ stratigraphic alignment. *EGUphere* 1–29 (2022).

788 **Acknowledgements**

789 We would like to express our gratitude to two anonymous reviewers whose thoughtful and constructive comments significantly
790 improved the overall quality of the paper. This work is Tipping Points in the Earth System (TiPES) contribution #180. This
791 study has been funded by the European Union’s Horizon 2020 research and innovation programme (grant agreement No.
792 820970). This is LDEO contribution.

793 **Author contributions statement**

794 W.B., D.D.R. and M.G.. outlined the manuscript, W.B. and D.D.R. collected the datasets, W.B. carried out the computations
795 and drew the plots, and W.B., D.D.R. and M.G. analyzed the results. W.B. drafted the manuscript and all authors reviewed and
796 finalized it.

797 **Competing interests**

798 The authors declare no competing interests.